AD_____

Award Number: W81XWH-09-1-0165

TITLE: Blocking FAK signaling in the tumor or stroma and effects
       on metastasis

PRINCIPAL INVESTIGATOR: David D. Schlaepfer, Ph.D.

CONTRACTING ORGANIZATION: University of California, San Diego
                          La Jolla, CA 92093-0621

REPORT DATE: April 2010

TYPE OF REPORT: Annual

PREPARED FOR: U.S. Army Medical Research and Materiel Command
               Fort Detrick, Maryland 21702-5012

DISTRIBUTION STATEMENT:

    X Approved for public release; distribution unlimited

REPORT DOCUMENTATION PAGE

1. REPORT DATE *(DD-MM-YYYY)*	2. REPORT TYPE	3. DATES COVERED *(From - To)*
01-04-2010	Annual	1 April 2009 – 31 MAR 2010

4. TITLE AND SUBTITLE

Blocking FAK signaling in the tumor or stroma and effects on metastasis

5a. CONTRACT NUMBER

5b. GRANT NUMBER
W81XWH-09-1-0165

5c. PROGRAM ELEMENT NUMBER

6. AUTHOR(S)
David D. Schlaepfer, Ph.D.
*
Email: dschlaepfer@ucsd.edu

5e. TASK NUMBER

5f. WORK UNIT NUMBER

7. PERFORMING ORGANIZATION NAME(S) AND ADDRESS(ES)

University of California, San Diego
*

La Jolla, CA 92093-0621

8. PERFORMING ORGANIZATION REPORT NUMBER

9. SPONSORING / MONITORING AGENCY NAME(S) AND ADDRESS(ES)
US Army Medical Research and
Material Command
Fort Detrick, MD 21702-5012

10. SPONSOR/MONITOR'S ACRONYM(S)

11. SPONSOR/MONITOR'S REPORT NUMBER(S)

12. DISTRIBUTION / AVAILABILITY STATEMENT
Approved for public release; distribution unlimited

13. SUPPLEMENTARY NOTES

14. ABSTRACT
FAK expression and activity are elevated during ovarian cancer progression and this is associated with a poor clinical prognosis. We have found that a new small molecular FAK inhibitor can block ovarian carcinoma tumor growth in mice without general toxicity. To determine the mechanism of action, we found that FAK activity selectively promotes the survival of tumor cells when grown under three-dimensional (3D) conditions as spheroids but not in normal adherent 2D culture. These results point to a novel role for FAK activity in generating anchorage-independent survival signals. We hypothesize that pharmacological inhibition of this novel FAK survival pathway may synergize with existing cytotoxic chemotherapies for ovarian cancer treatment.

15. SUBJECT TERMS
Cell survival, tyrosine kinase, tumor growth, ovarian cancer, FAK

16. SECURITY CLASSIFICATION OF:			17. LIMITATION OF ABSTRACT	18. NUMBER OF PAGES	19a. NAME OF RESPONSIBLE PERSON USAMRMC
a. REPORT U	b. ABSTRACT U	c. THIS PAGE U	UU	20	19b. TELEPHONE NUMBER *(include area code)*

Table of Contents

Introduction

Ovarian cancer is usually advanced at diagnosis, due to the propensity to shed malignant cells that attach to and invade through the peritoneal wall or to other organs. Focal adhesion kinase (FAK) is a cytoplasmic protein-tyrosine kinase activated by integrin signals within tumor cells. FAK also functions as a key signaling intermediate downstream of the VEGF receptor in endothelial cells (ECs) in promoting angiogenesis. What remains undetermined is the role of FAK activity in tumor versus stromal cells in promoting tumor progression. In this proposal, we will study the role of FAK within ID8 ovarian carcinoma cells that were isolated from C57Bl6 mouse ovary epithelium and spontaneously transformed by passage in culture. Epithelial-stromal interactions of ID8 cells with the microenvironment play important roles in promoting cell proliferation, survival and tumorigenicity. We will test whether the inhibition of FAK selectively within tumor cells, stromal ECs, or both will affect ovarian carcinoma tumor progression. Our proposal will combine genetic (shRNA knockdown and FAK re-expression in ID8 cells), pharmacological (we have co-developed a new small molecule FAK inhibitors), and a novel syngeneic mouse model (ID8 cells can be grown in C57BL6 mice with an inducible conditional knockout of FAK within ECs, i-EC-FAK-KO) to determine whether blocking FAK signaling in tumor or stroma will affect tumor growth and metastasis. Our proposal is based upon the hypothesis that targeting a common signaling protein activated within ovarian carcinoma tumor cells and stromal ECs may be a highly efficacious strategy to block tumor progression and metastasis. We will test whether FAK fits this profile.

Body

During mouse development, loss of FAK expression in ECs is connected to a block in cell proliferation caused by up-regulated p53 tumor suppressor activity in promoting the expression of targets such as the p21 cyclin-dependent kinase inhibitor [1, 2]. However in adult mice, EC-specific FAK inactivation is associated with increased Pyk2 expression that enables growth factor-stimulated angiogenesis in the absence of FAK [3]. Elevated Pyk2 expression also occurs in vitro upon FAK inactivation in primary fibroblasts and ECs [3, 4]. However, the molecular roles that Pyk2 performs upon FAK inactivation remain unclear. We hypothesize that compensatory Pyk2 expression is part of an adaptive or intrinsic cell survival mechanism. In a recent publication from our group [5], we establish that Pyk2 in both normal and tumor cells acts to regulate levels of the p53 tumor suppressor protein controlling both cell proliferation and survival. Pyk2 regulation of p53 occurs in a kinase-independent manner via Pyk2 N-terminal band 4.1, ezrin, radixin, moesin (FERM) domain nuclear translocation. Pyk2 FERM forms a complex with p53 and promotes enhanced Mdm2-dependent p53 ubiquitination and subsequent degradation.

As ID8 cells express FAK, Pyk2, and wildtype p53, we needed to determine whether knockdown of FAK or Pyk2 would effect ID8 cell proliferation or survival. We found that FAK shRNA knockdown did not result in detectable changes in ID8 p53 or p21 levels (Fig. 1A) nor did it affect ID8 cell growth (data not shown) or cell cycle progression (Fig. 1C). In contrast, Pyk2 shRNA knockdown triggered elevated p53 and p21 levels (Fig. 1A), inhibited ID8 cell proliferation (Fig. 1B), and was associated with an increased percentage of ID8 cells in G0/G1 and decreased percentage in S phase of the cell cycle compared to Scr shRNA controls (Fig. 1C). To prove the specificity of the Pyk2 knockdown results, human Myc-tagged Pyk2
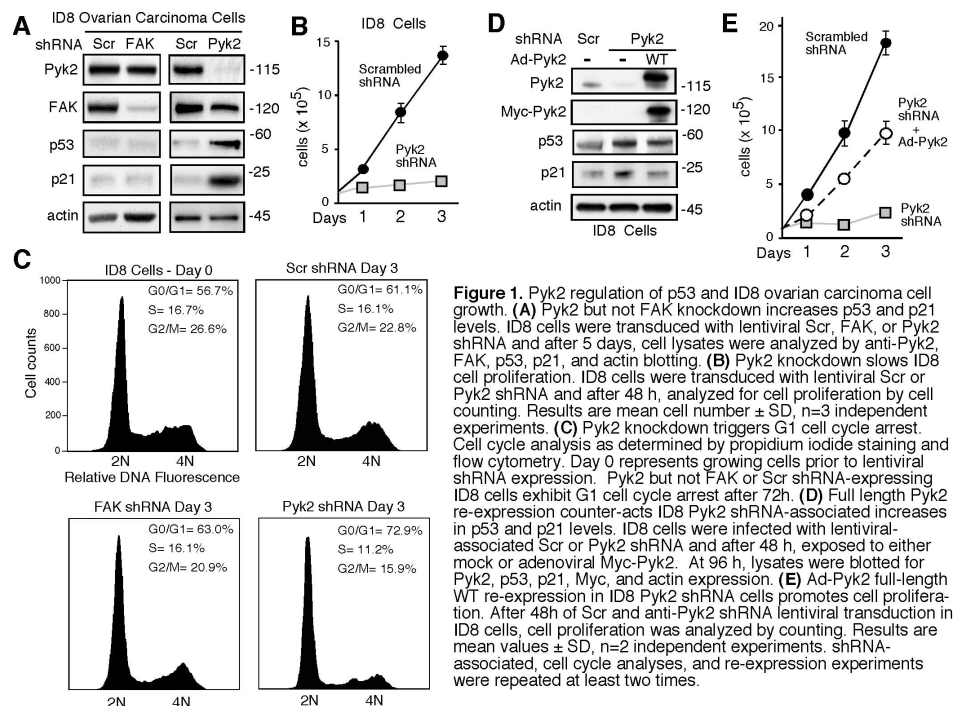

Figure 1. Pyk2 regulation of p53 and ID8 ovarian carcinoma cell growth. (A) Pyk2 but not FAK knockdown increases p53 and p21 levels. ID8 cells were transduced with lentiviral Scr, FAK, or Pyk2 shRNA and after 5 days, cell lysates were analyzed by anti-Pyk2, FAK, p53, p21, and actin blotting. (B) Pyk2 knockdown slows ID8 cell proliferation. ID8 cells were transduced with lentiviral Scr or Pyk2 shRNA and after 48 h, analyzed for cell proliferation by cell counting. Results are mean cell number ± SD, n=3 independent experiments. (C) Pyk2 knockdown triggers G1 cell cycle arrest. Cell cycle analysis as determined by propidium iodide staining and flow cytometry. Day 0 represents growing cells prior to lentiviral shRNA expression. Pyk2 but not FAK or Scr shRNA-expressing ID8 cells exhibit G1 cell cycle arrest after 72h. (D) Full length Pyk2 re-expression counter-acts ID8 Pyk2 shRNA-associated increases in p53 and p21 levels. ID8 cells were infected with lentiviral-associated Scr or Pyk2 shRNA and after 48 h, exposed to either mock or adenoviral Myc-Pyk2. At 96 h, lysates were blotted for Pyk2, p53, p21, Myc, and actin expression. (E) Ad-Pyk2 full-length WT re-expression in ID8 Pyk2 shRNA cells promotes cell proliferation. After 48h of Scr and anti-Pyk2 lentiviral transduction in ID8 cells, cell proliferation was analyzed by counting. Results are mean values ± SD, n=2 independent experiments. shRNA-associated, cell cycle analyses, and re-expression experiments were repeated at least two times.

was re-expressed in the murine Pyk2 shRNA-expressing ID8 cells. Pyk2 re-expression reversed the rise in p53 and p21 levels (Fig. 1D) and also promoted ID8 cell proliferation (Fig. 1E) compared to Pyk2 shRNA-

expressing ID8 cells. Although it remains unclear why Pyk2 (and not FAK) is connected to p53 regulation in ID8 cells, these results are a key foundational step that will allow us to effectively knockdown FAK expression without affecting ID8 cell growth in culture. This will be important for future experiments where we will re-express kinase-inactive FAK back into the ID8 knockdown cells.

During ovarian carcinoma tumor cell progression, cells can dissociate from the primary tumor and grow as multi-cellular spheroids within the peritoneal space [6]. As directly part of the Statement of Work, one of the first goals was to determine the role of FAK activity in promoting ID8 cell growth in vitro and as ascites-associated tumors in vivo. We have accomplished this goal through the use of a new small molecule FAK inhibitor (PND-1186) developed by Poniard Pharmaceuticals, Inc. We have found that PND-1186 selectively promotes breast carcinoma cell apoptosis in 3D environments without effects on cell growth-survival in normal adherent culture conditions [7]. PND-1186 also blocks spontaneous breast to lung metastasis in pre-clinical tumor models [8]. Therefore, we tested PND-1186 effects on murine ID8 ovarian carcinoma cell growth *in vitro* and *in vivo* (Fig. 2). In suspended cell culture as spheroids, 0.1, 0.4, and 1.0 µM PND-1186 significantly inhibited ID8 cell number at 72 h (Fig. 2A) and resulted in a dramatic reduction in viable cells after 15 days (Fig. 2B). To determine if low levels of PND-1186 could affect ID8 growth in vivo, dsRed fluorescently-labeled ID8 cells were intraperitoneally-injected into C57Bl6 mice and after 11 days, mice were provided 5% sucrose (control) or 0.5 mg/ml PND-1186 in 5% sucrose in lieu of drinking water on an *ad libitum* basis. No adverse effects and no body weight loss were noted with PND-1186 administration. After 30 treatment days, mice with PND-1186 in the drinking water did not exhibit swollen abdomens as did control mice (Fig. 2C). This corresponded with a lower number of ascites-associated cells (Fig. 2D) and the >2-fold inhibition of FAK pY397 by 0.5 mg/ml PND-1186 administration compared to 5% sucrose controls (Fig. 2E and F). In addition to inhibiting ascites-associated ID8 spheroid growth, PND-1186-treated mice showed significantly fewer tumor nodules within the peritoneal space as detected by *in vivo* dsRed fluorescence imaging (Fig. 2G and H). These results show that low level PND-1186 administration inhibits the growth of ovarian carcinoma cells *in vitro* and *in vivo*. The selective effects on PND-1186 in promoting apoptosis of cells in three dimensional environments points to a novel role for FAK activity in generating anchorage-independent survival signals. The manuscript encompassing this work (Tanjoni et al.) has been accepted for publication and is in the Appendix.
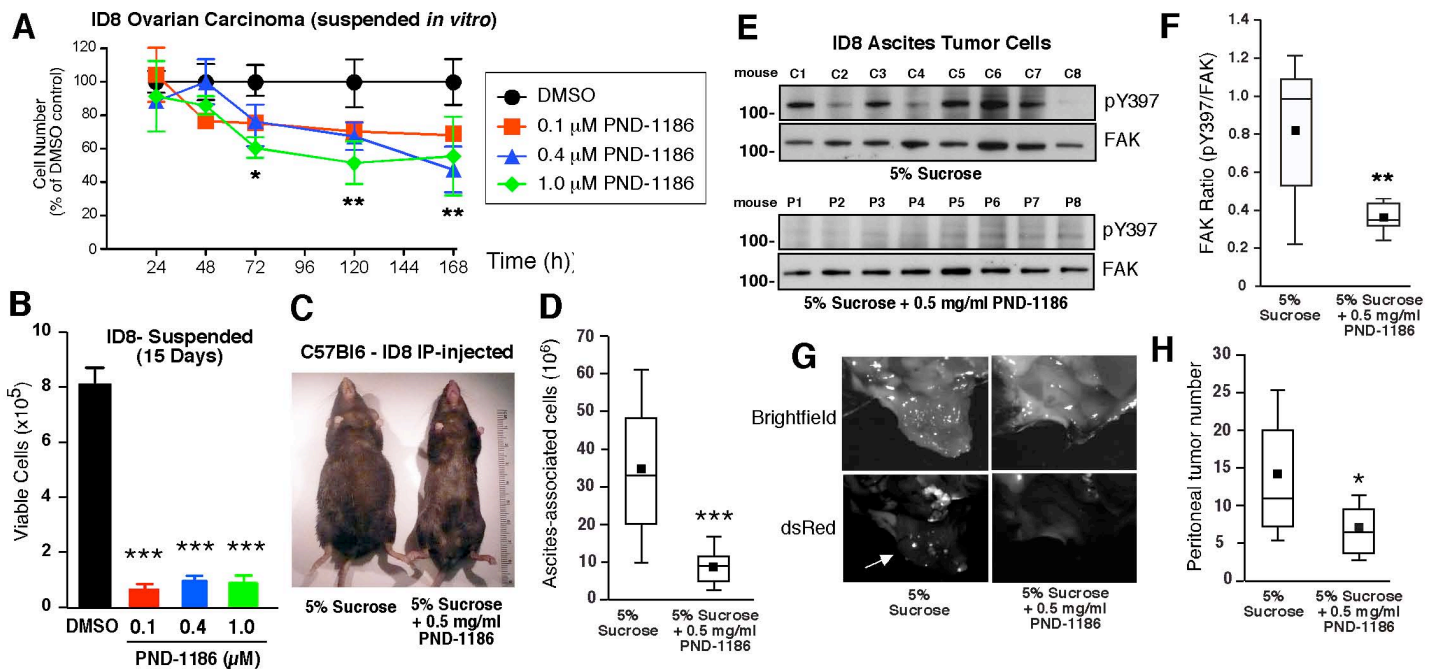

Figure 8. PND-1186 inhibits ovarian carcinoma tumor growth. **(A and B)** ID8 cells were plated under non-adherent conditions (poly-HEMA-coated plate) in the presence of DMSO or the indicated amounts of PND-1186 and enumerated from 24 to 168 h as indicated. **(B)** Viable cell numbers were determined by trypan blue exclusion and counting using a Vi-Cell analyzer after 15 days. **(C)** Representative images of C57Bl6 mice injected (intraperitoneal, IP) with dsRed-labeled ID8 cells after 46 days provided 5% sucrose (control) or 0.5 mg/ml PND-1186 in 5% sucrose ad libitum as drinking water for 30 days. **(D)** Ascites was collected, peritoneal cavity washed with saline, and total cell numbers enumerated from ID8 IP-injected mice. **(E)** Evaluation of FAK phosphorylation in ascites-associated cells as determined by anti-FAK followed by phospho-specific anti-FAK pY397 immunoblotting. **(F)** Ratio of pY397 phosphorylated FAK to total FAK levels in ascites cells as determined by densitometry using Image J (n=8 per group). **(G)** Representative brightfield and fluorescent images of peritoneal tissue from C57Bl6 mice IP-injected with dsRed-labeled ID8 cells after 46 days provided 5% sucrose (control) or 0.5 mg/ml PND-1186. Arrow indicates dsRed-positive tumor nodules in control mice. (H) Peritoneal-associated tumors were quantified by counting (n=8 per group). Values are means (+/- SD) performed in triplicate and significance was determined by ANOVA (*p < 0.05; **p<0.001, ***p<0.0001 versus control). Box-and-whisker diagrams show the distribution of the data: square, mean; bottom line, 25th percentile; middle line, median; top line, 75th percentile; and whiskers, 5th or 95th percentiles.

5

Key Research Accomplishments

- Determined the role of FAK and Pyk2 for growth and survival of ID8 cells.
- Selective inhibition of ID8 cell growth by FAK kinase inhibition in suspension or 3D culture.
- Proof-of-principal testing of oral delivery of FAK inhibitor in blocking ovarian carcinoma tumor growth in mice.

Reportable Outcomes

1. Manuscript Publication

Tanjoini, I., Walsh, C., Uryu, S., Tomar, A., Nam, J.O., Mielgo, A., Lim, S.T., Liang, C., Koenig, M., Patel, N., Kwok, C., McMahon, G., Stupack, D.G., and Schlaepfer, D.D. (2010). PND-1186 FAK inhibitor selectively promotes tumor cell apoptosis in three-dimensional environments. *Cancer Biol. Therapy* (in press).

Conclusion

FAK expression and activity are elevated during ovarian cancer progression and this is associated with a poor clinical prognosis. We have found that a new small molecular FAK inhibitor can block ovarian carcinoma tumor growth in mice without general toxicity. To determine the mechanism of action, we found that FAK activity selectively promotes the survival of tumor cells when grown under three-dimensional (3D) conditions as spheroids but not in normal adherent 2D culture. These results point to a novel role for FAK activity in generating anchorage-independent survival signals. We hypothesize that pharmacological inhibition of this novel FAK survival pathway may synergize with existing cytotoxic chemotherapies to enhance effectiveness or prevent resistance to ovarian cancer treatments.

References

1. Ilic, D., et al., 2003. Focal adhesion kinase is required for blood vessel morphogenesis. Circ. Res. 92: 300-307.
2. Lim, S.T., et al., 2008. Nuclear FAK promotes cell proliferation and survival through FERM-enhanced p53 degradation. Mol Cell. 29: 9-22.
3. Weis, S.M., et al., 2008. Compensatory role for Pyk2 during angiogenesis in adult mice lacking endothelial cell FAK. J. Cell Biol. 181: 43-50.
4. Lim, Y., et al., 2008. PyK2 and FAK connections to p190Rho guanine nucleotide exchange factor regulate RhoA activity, focal adhesion formation, and cell motility. J Cell Biol. 180: 187-203.
5. Lim, S.T., et al., 2009. PYK2 inhibition of p53 as an adaptive and intrinsic mechanism facilitating cell proliferation and survival. J Biol Chem. 285: 1743-1753.
6. Shield, K., et al., 2009. Multicellular spheroids in ovarian cancer metastases: Biology and pathology. Gynecol Oncol. 113: 143-148.
7. Tanjoni, I., et al., 2010. PND-1186 FAK inhibitor selectively promotes tumor cell apoptosis in three-dimensional environments. Cancer Biology & Therapy. (in press).
8. Walsh, C., et al., 2010. Oral delivery of PND-1186 FAK inhibitor decreases spontaneous breast to lung metastasis in pre-clinical tumor models. Cancer Biology & Therapy (in press).

PND-1186 FAK inhibitor selectively promotes tumor cell apoptosis in three-dimensional environments

Isabelle Tanjoni,[1,†] Colin Walsh,[1,†] Sean Uryu,[1] Alok Tomar,[1] Ju-Ock Nam,[1] Ainhoa Mielgo,[2] Ssang-Taek Lim,[1] Congxin Liang,[3] Marcel Koenig,[3] Connie Sun,[4] Neela Patel,[4] Cheni Kwok,[4] Gerald McMahon,[4] Dwayne G. Stupack,[2,‡] and David D. Schlaepfer[1,*]

[1]Departments of Reproductive Medicine; University of California San Diego Moores Cancer Center; La Jolla, CA USA; [2]Departments of Pathology; University of California San Diego Moores Cancer Center; La Jolla, CA USA, [3]Scripps Florida; Jupiter, FL USA; [4]Poniard Pharmaceuticals Inc.; South San Francisco, CA USA

[†]These authors contributed equally to this work.

[‡]Co-corresponding authors

Tumor cells can grow in an anchorage-independent manner. This is mediated in part through survival signals that bypass normal growth restraints controlled by integrin cell surface receptors. Focal adhesion kinase (FAK) is a cytoplasmic protein-tyrosine kinase that associates with integrins and modulates various cellular processes including growth, survival and migration. As increased FAK expression and tyrosine phosphorylation are associated with tumor progression, inhibitors of FAK are being tested for anti-tumor effects. Here, we analyze PND-1186, a substituted pyridine reversible inhibitor of FAK activity with a 50% inhibitory concentration (IC_{50}) of 1.5 nM in vitro. PND-1186 has an IC_{50} of ~100 nM in breast carcinoma cells as determined by anti-phospho-specific immunoblotting to FAK Tyr-397. PND-1186 did not alter c-Src or p130Cas tyrosine phosphorylation in adherent cells, yet functioned to restrain cell movement. Notably, 1.0 μM PND-1186 (>5-fold above IC_{50}) had limited effects on cell proliferation. However, under non-adherent conditions as spheroids and as colonies in soft agar, 0.1 μM PND-1186 blocked FAK and p130Cas tyrosine phosphorylation, promoted caspase-3 activation, and triggered cell apoptosis. PND-1186 inhibited 4T1 breast carcinoma subcutaneous tumor growth correlated with elevated tumor cell apoptosis and caspase 3 activation. Addition of PND-1186 to the drinking water of mice was well tolerated and inhibited ascites- and peritoneal membrane-associated ovarian carcinoma tumor growth associated with the inhibition of FAK Tyr-397 phosphorylation. Our results with low-level PND-1186 treatment support the conclusion that FAK activity selectively promotes tumor cell survival in three-dimensional environments.

Introduction

Focal adhesion kinase (FAK) is a cytoplasmic protein-tyrosine kinase that associates with both integrins and growth factor receptors in the control of cell motility and survival.[1,2] Integrin binding to extracellular matrix promotes FAK activation connected to the regulation of various downstream signaling pathways involved in cell shape changes and motility.[3] In many tumors and transformed cell lines, FAK expression and tyrosine phosphorylation are elevated.[4-6] Knockdown of FAK within tumor cells or mouse tumor models where FAK expression is inactivated have shown that FAK is important for breast carcinoma tumor progression.[7-11] Importantly, studies where FAK activity was inhibited through either a dominant-negative FAK protein fragment or comparisons of tumor cells expressing kinase-inactive FAK show that FAK activity is needed for breast

*Correspondence to: David D. Schlaepfer; Email: dschlaepfer@ucsd.edu

A

PND-1186 Profile

In vitro

Purified FAK kinase: IC_{50} = 1.5 nM

Kinase Selectivity: high

Cellular Inhibition: IC_{50} = ~100 nM

Solubility: 22 mg/mL in H_2O

Microsome stability: $t_{1/2}$ (human) = 31 min

In vivo

Protein Binding: 97% (Human and Mouse)

Oral Bioavailability - Rat: 53-61%, dose proportional

Oral Bioavailability - Mouse: 13-20%, dose proportional

Tolerability: ≥ 500 mg/kg in mice (p.o.)

B

Kinase Profile Analyses

	PND-1186 (0.1 μM)	PND-1186 (1 μM)
Abl	104	112
ACK1	56	16
ALK	145	127
Aurora-A	69	8
CDK2/cyclinA	91	42
CHK1	109	105
CK1g1	111	107
cKit	119	122
c-RAF	142	150
c-SRC	98	72
DAPK1	104	97
EGFR	99	106
EphA1	81	108
FAK	38	0
FGFR1	98	97
Flt3	28	8
Fyn	99	78
IGF-1R	123	110
IR	84	40
JAK2	116	96
KDR	118	107
Lck	76	32
MAPK1	78	58
MEK1	79	79
NEK6	110	107
p70S6K	95	97
PDGFRb	98	105
PKA	114	111
PKCa	101	96
Ret	86	67
ROCK-1	96	90
Tie2	97	74
TrkA	80	27
ZAP-70	70	75

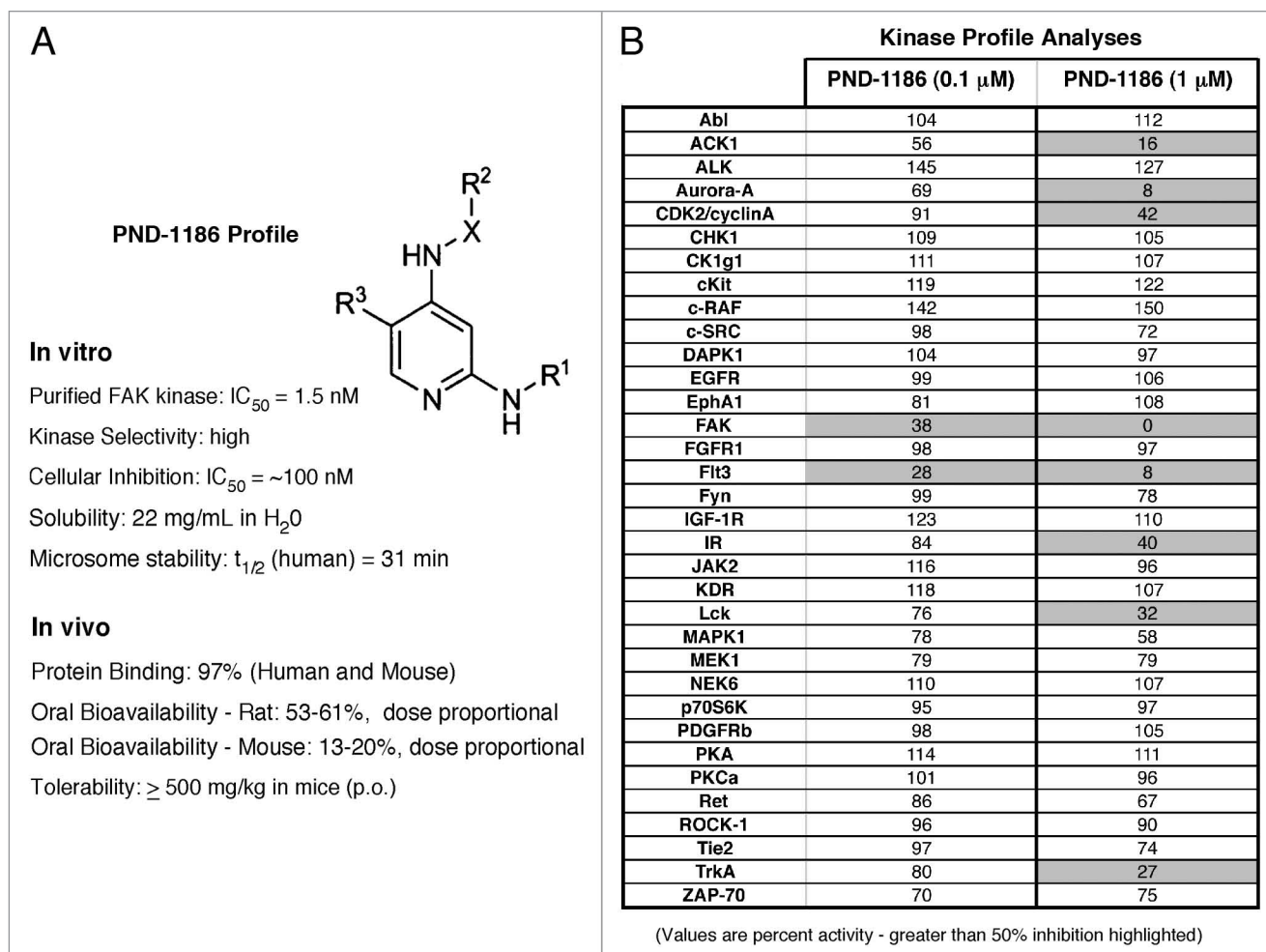(Values are percent activity - greater than 50% inhibition highlighted)

Figure 1. Properties of PND-1186 and selective FAK inhibition. (A) PND-1186 is comprised of 2,4-diamino-pyridine-based scaffold. For the partial PND-1186 structure presented, X is a bond or (C₁-C₃)alkyl comprising 0–1 heteroatom selected from the group consisting of N, O, S(O) and S(O)₂, wherein the (C₁-C₃)alkyl is substituted with 0–1 hydroxy, halo, (C₁-C₃)alkoxy, (C₁-C₃)alkylamino or (C₁-C₃)₂dialkylamino groups. R¹ and R² are 5–12 membered monocyclic, bicyclic or polycyclic, aromatic or partially aromatic rings. R³ is a trifluoromethyl, halo, nitro or cyano; salt, tautomer, solvate, hydrate, or a prodrug thereof. ELISA-based IC_{50} inhibition of recombinant FAK kinase activity was 1.5 nM and cellular inhibition was determined by anti-phospho-specific Tyr-397 FAK immunoblotting. PND-1186 is water-soluble, exhibits favorable microsome stability, is highly protein bound in plasma (97%), exhibits dose proportionality in bioavailability, and high level oral administration (p.o) is not toxic to mice. (B) Relative inhibition of various kinases with 0.1 or 1.0 μM PND-1186 addition as performed by the Millipore Kinase Profiler Service. Values are percent activity, greater than 50% inhibition is highlighted in grey. At 0.1 μM, PND-1186 showed high selectivity for FAK and Flt3 inhibition.

carcinoma metastasis.[12,13] As FAK is connected to multiple cell surface receptors and downstream signaling pathways, pharmacological inhibition of FAK activity may affect multiple aspects of tumor progression.[14]

ATP-competitive small molecule inhibitors to FAK have been developed by Novartis (TAE-226)[15] and Pfizer (PF-573,228, PF-562,271).[16,17] Additionally, compounds (such as Y15) have been identified that block access to the major FAK tyrosine-397 autophosphorylation and Src-family kinase binding to FAK.[18] TAE-226, which is also a high affinity inhibitor of insulin-like growth factor receptor signaling,[19] can prevent tumor cell growth in vitro and in vivo.[15,19-21] Y15 promotes cell apoptosis and also inhibits tumor growth at concentrations that are 10 to 100-fold above the 50% inhibitory concentration (IC_{50}) for FAK inhibition.[18,22] In contrast, PF-573,228 and PF-562,271 are highly selective for

FAK and the related Pyk2 kinase,[16,17] yet do not block cell proliferation or promote tumor cell apoptosis in vitro at 10-fold levels above the IC_{50} for FAK. Thus, FAK activity does not appear essential for cell proliferation.[23] However, PF-562,271 prevents growth of subcutaneous human tumor xenografts, and this is associated with decreased microvascular density and increased tumor apoptosis.[17] Although PF-562,271 blocks endothelial cell branching in chicken chorioallantoic membrane and mouse aortic ring angiogenesis assays,[23,24] it remains unclear whether these actions are connected to the mechanism(s) associated with PF-562,271-induced tumor cell apoptosis.

Herein, we present the characterization of a new highly-specific small molecule inhibitor to FAK. PND-1186 has an IC_{50} of 1.5 nM to recombinant FAK and ~0.1 μM in breast carcinoma cells as determined by anti-phospho-specific immunoblotting to
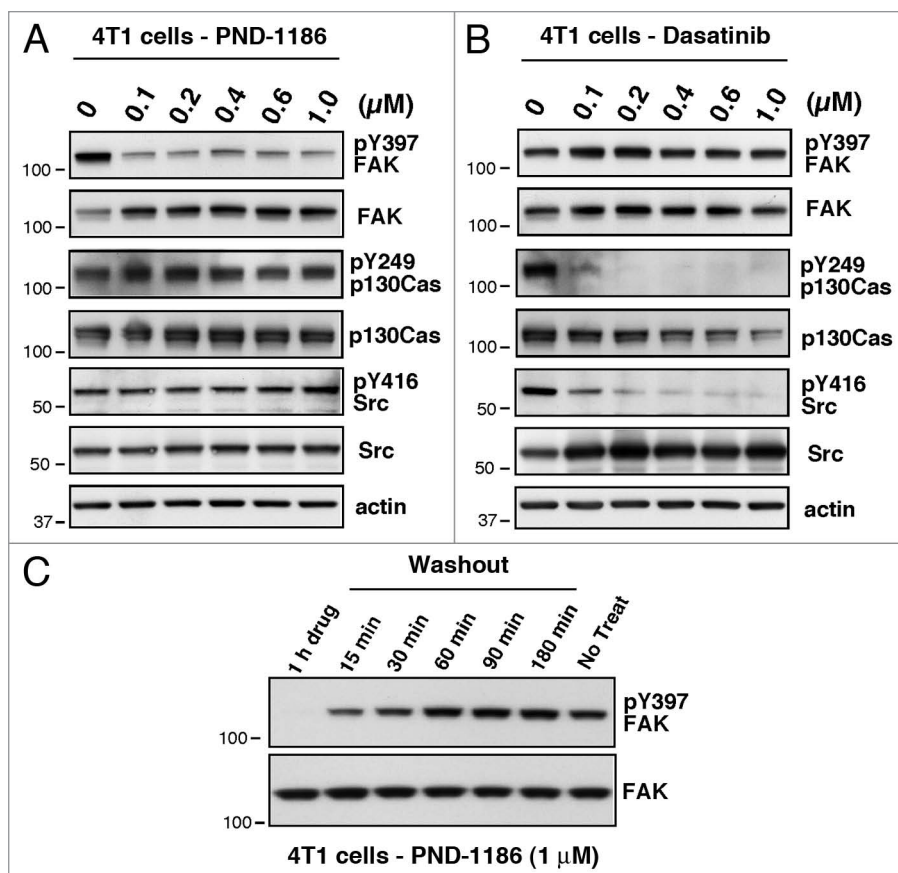
Figure 2. PND-1186 inhibitory effects differ from Dasatinib (Src inhibition). Effect of PND-1186 on FAK, c-Src and p130Cas tyrosine phosphorylation. 4T1 cells were seeded at 70% confluency on tissue culture plates coated with 10 µg/ml fibronectin. Cells were treated with vehicle (DMSO) or increasing (A) PND-1186 or (B) Dasatinib (LC Labs Inc.) addition for 1 h. Shown is total FAK, p130Cas, Src or actin levels in cell lysates. Phospho-specific immunoblotting was performed in parallel for changes in FAK or Src activity (pY397 FAK or pY416 Src) and p130Cas tyrosine phosphorylation (pY249 p130Cas). (C) Time course of FAK pY397 phosphorylation in 4T1 cells after 1 h treatment (PND-1186, 1 µM) followed by PBS wash. Protein lysates were made at indicated times after PBS wash.

Results

Properties of PND-1186 and selectivity of FAK inhibition. PND-1186 has a 2,4-diamino-pyridine primary ring structure (**Fig. 1**). Using the recombinant FAK kinase domain as a glutathione-S-transferase (GST) fusion protein in an in vitro kinase assay (**Suppl. Fig. 1**), PND-1186 inhibited FAK activity with IC$_{50}$ of 1.5 nM. The selectivity of PND-1186 was evaluated using the Millipore KinaseProfiler Service. In this screen with recombinant protein kinases, 0.1 µM PND-1186 displayed specificity for FAK as well as Flt3 (FMS-like tyrosine kinase 3) kinase inhibition. At a higher PND-1186 levels (1 µM), FAK and Flt3 had negligible activity and other kinases including ACK1 (activated Cdc42-associated tyrosine kinase 1), Aurora-A, CDK2 (cyclin-dependent kinase 2)/cyclin A, insulin receptor (IR), Lck (lymphocyte-specific protein tyrosine kinase) and TrkA (tropomyosin-related kinase A) were inhibited greater than 50% (**Fig. 1**). Flt3 expression is found in cells of hematopoietic origin and is not detectably expressed in 4T1, MDA-MB-231 or ID8 cells used herein.

PND-1186 inhibition of FAK is distinct from effects of Src PTK inhibitors. FAK acts as both a signaling kinase and cell adhesion-associated scaffold within tumor cells to coordinate the positional recruitment and phosphorylation of various cytoskeletal-associated proteins such as p130Cas and paxillin.[1,25] Increased FAK autophosphorylation at Y397 is a marker of FAK activation. Integrin-mediated Y397 FAK phosphorylation can promote Src-family tyrosine kinase binding to FAK and can lead to FAK-mediated c-Src activation.[26] As both FAK and c-Src can phosphorylate common downstream targets such as p130Cas,[27] it remains undetermined whether the effects of FAK and/or c-Src inhibition will yield differential results on downstream target phosphorylation events.

In murine 4T1 breast carcinoma cells, we previously showed that FAK promotes an invasive and metastatic cell phenotype.[13] Increasing concentrations of PND-1186 (0.1 to 1.0 µM) added to 4T1 cells inhibited FAK Tyr-397 phosphorylation (pY397) and resulted in elevated levels of total FAK protein within 1 h (**Fig. 2A**). Similar results were obtained by PND-1186 addition to human MD-MBA-231 breast carcinoma cells and murine ID8 ovarian carcinoma cells (data not shown). The cellular IC$_{50}$ for FAK pY397 inhibition was determined as ~0.1 µM PND-1186 by densitometry analyses and maximal reduction of FAK pY397 phosphorylation was ~80% (**Fig. 2A**). These results are consistent

FAK Tyr-397. Surprisingly, PND-1186 concentrations up to 1.0 µM did not inhibit p130Cas (130 kDa Crk-associated substrate) or c-Src tyrosine phosphorylation within adherent cells, and had limited effects on cell growth in two-dimensional culture. However, PND-1186 inhibited breast carcinoma cell motility in a dose-dependent fashion.

A hallmark of cancer is the ability to grow in an anchorage-independent manner. We show that 0.1 µM PND-1186 is sufficient to trigger 4T1 breast carcinoma and ID8 ovarian carcinoma cell apoptosis when grown under suspended, spheroid or soft-agar conditions. This was associated with the inhibition of both FAK and p130Cas tyrosine phosphorylation, supporting the hypothesis that a FAK-p130Cas survival pathway facilitates three-dimensional (3D) cell growth. PND-1186 inhibits 4T1 subcutaneous tumor growth and is associated with increased tumor cell apoptosis. Similarly, low-dose drinking water administration of PND-1186 inhibited ID8 ovarian ascites-associated tumor burden without murine weight loss or morbidity. Our results support the notion that FAK activity plays a novel role in promoting 3D cell survival.

A

4T1 Scratch-wound motility

DMSO

PND-1186
1 µM

0 h   11 h   22 h
(time-lapse series of images)

B

Percent wound closure

DMSO   PND-1186
(1 µM)

*

C

Motility - MilliCell Chamber

Percent of Control

p<0.05

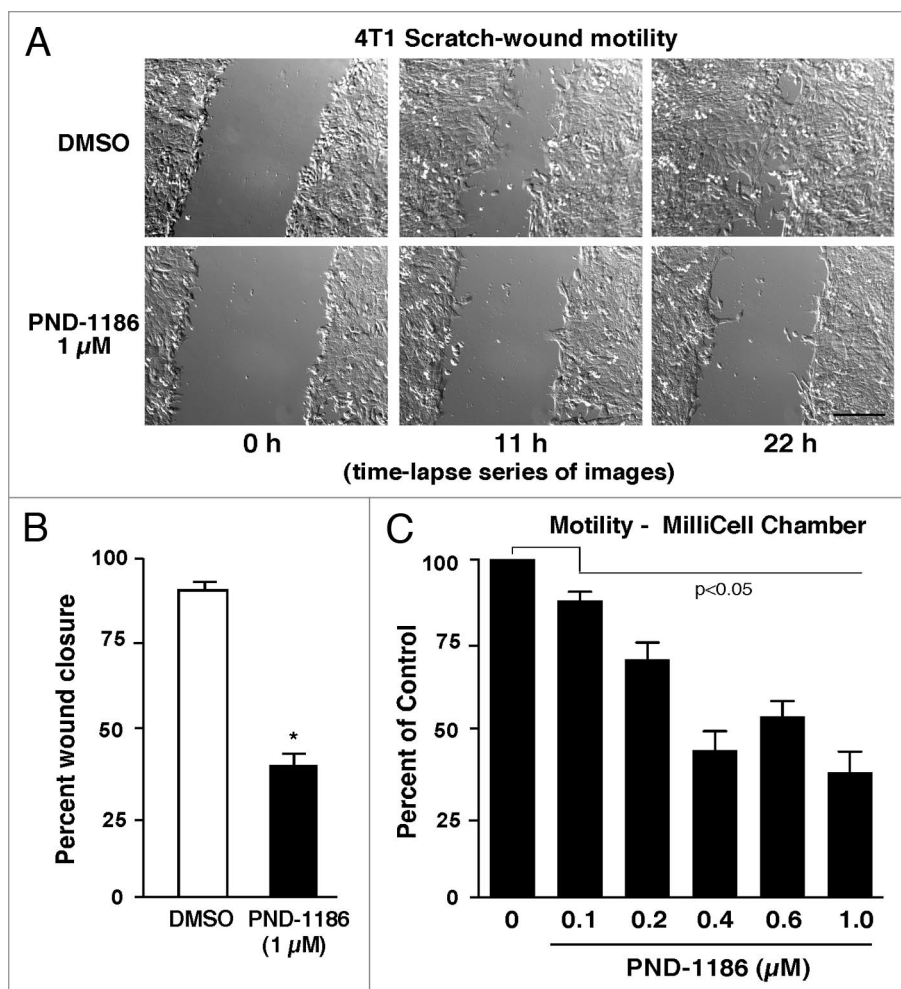0   0.1   0.2   0.4   0.6   1.0

PND-1186 (µM)

Figure 3. PND-1186 restrains 4T1 breast carcinoma motility. Confluent monolayer of 4T1 cells were wounded and photographed for 22 h via time lapse microscopy in the presence of vehicle (DMSO) or 1 µM PND-1186. (A) Representative images from wound assay at 0, 11 and 22 h are shown, scale bar is 250 µm. (B) Quantification of time-lapse images from one representative experiment in triplicate. Percent wound closure was determined using Image J and results are mean +/- SD. (C) Cells were pretreated (1 h) with vehicle or the indicated concentrations of PND-1186 then plated on fibronectin-coated MilliCell transwells and allowed to migrate for 4 h in the presence of drug. 10% FBS was used as a chemo-attractant. Results are percent of DMSO control (+/-SD, standard deviation) performed in triplicate (*p < 0.05 versus DMSO control using ANOVA). PND-1186 did not affect cell binding to fibronectin.

2B). Notably, dasatinib did not affect FAK pY397 levels (**Fig. 2B**) and similar results were obtained using MD-MBA-231 cells or another Src inhibitor such as 4-amino-5-(4-methylphenyl)-7-(*t*-butyl) pyrazolo[3,4-*d*]-pyrimidine or commonly known as PP1 (data not shown). Taken together, these results show that PND-1186 potently inhibits FAK phosphorylation in a reversible manner and that Src pY416 and p130Cas pY249 phosphorylation are dependent on Src but not FAK activity in adherent 4T1 cells.

PND-1186 inhibits 4T1 breast carcinoma motility in vitro. FAK expression is elevated in invasive humans cancers[14] and FAK signaling promotes directional cell movement.[2,3] To assess if PND-1186 would inhibit 4T1 cell migration, time lapse wound healing assays were performed in the presence of DMSO (dimethyl sulfoxide, control) or 1 µM PND-1186 (**Fig. 3A and Suppl. Videos 1 and 2**) for 22 h. PND-1186 prevented 4T1 cell movement and this was associated with the lack of protrusion formation and the infrequency of 4T1 edge cell separation from the collective monolayer. No evidence of 4T1 cell detachment or death was observed with 1 µM PND-1186 over 22 h and notably, cells were visualized undergoing cell division in the presence of 1.0 µM PND-1186 (**Suppl. Video-2**). Quantitation of several wound regions over 22 h revealed that DMSO-treated 4T1 cells showed 89% wound closure whereas PND-1186-treated cells had only 40% closure (**Fig. 3B**).

To validate the wound assay results, Millicell chamber motility assays were performed with membranes coated with fibronectin and serum added as a chemotaxis stimulus (**Fig. 3C**). Addition of PND-1186 to the Millicell motility assay prevented 4T1 cell movement in a dose-dependent fashion with ~50 to 60% maximal inhibition at 0.4 µM PND-1186 addition for 4 h. Importantly, PND-1186 did not affect 4T1 cell adhesion to fibronectin, as did dasatinib addition at sub-micromolar levels (data not shown). These results support the importance of FAK activity in promoting 4T1 cell motility.

Nanomolar PND-1186 levels promote 4T1 apoptosis in suspended but not adherent conditions. At 1 µM, the TAE-226 FAK inhibitor prevents glioma cell proliferation in vitro,[15,19] yet the PF-573,228 FAK inhibitor does not block fibroblast or prostate carcinoma cell growth at 1 µM or 10-fold levels above the IC$_{50}$ for FAK.[16] Thus, FAK activity may not be tightly associated with the regulation of cell proliferation. To determine effects on

with PF-573,228 inhibition of FAK in A431 epithelial carcinoma cells[16] and residual levels of FAK Y397 phosphorylation in the presence of PND-1186 may reflect FAK phosphorylation in trans by other protein-tyrosine kinases.[28]

PND-1186 inhibition of FAK was reversible as washout experiments showed that FAK pY397 phosphorylation fully recovered within 60 min (**Fig. 2C**). Surprisingly, PND-1186 addition to 1 µM did not affect c-Src activity as determined by phosphos-specific antibody reactivity to Src Tyr-416 (pY416) or p130Cas Tyr-249 (pY249) phosphorylation in adherent 4T1 cells (**Fig. 2A**). In contrast, when dasatinib (BMS-354825) was added to 4T1 cells (inhibiting both Abelson murine leukemia viral oncogene homolog 1, Abl and Src-family kinases), both Src pY416 and p130Cas pY249 were reduced in a dose-dependent manner (**Fig.**
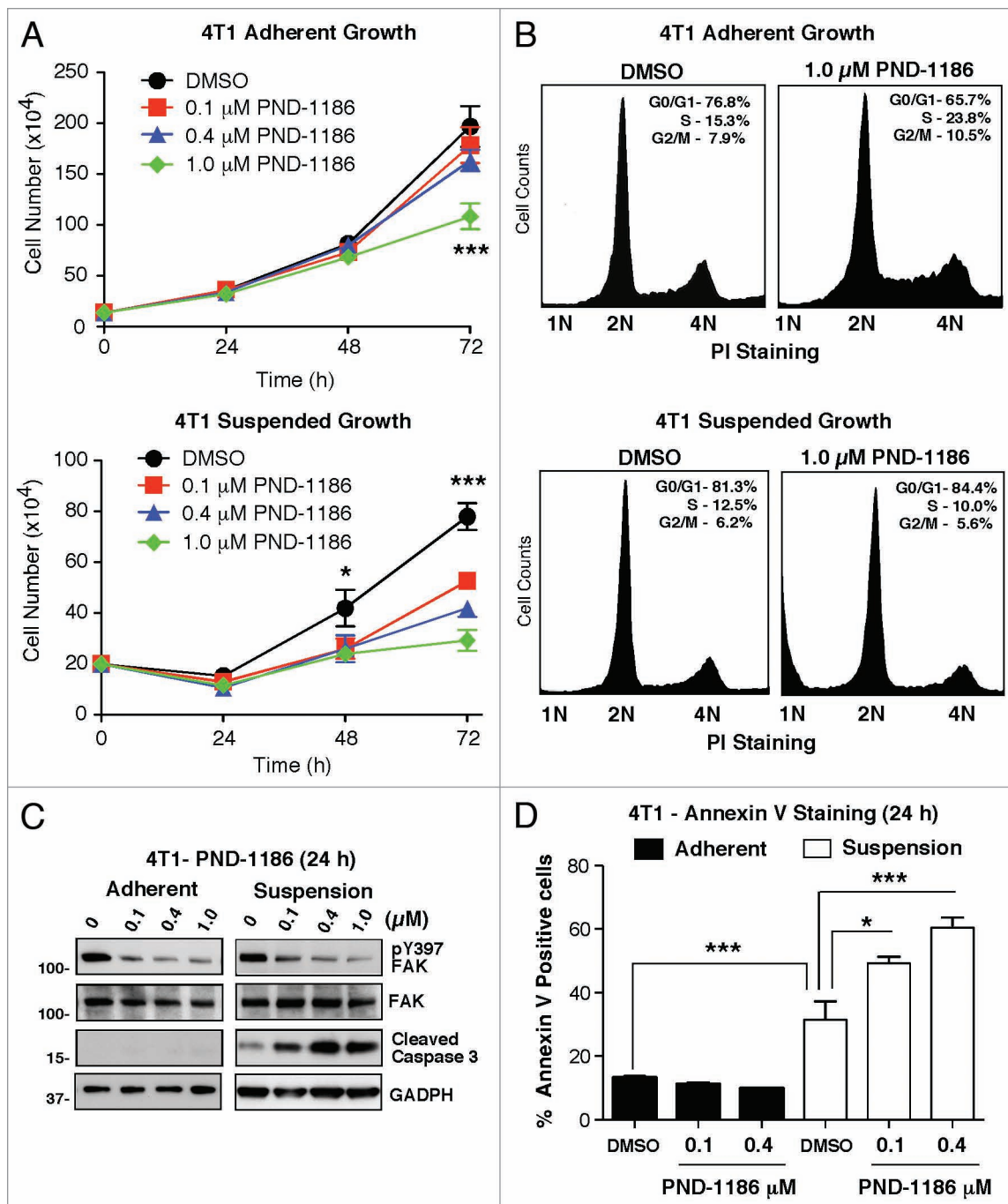
Figure 4. Selective 4T1 cell apoptosis in suspension at low PND-1186 levels. (A) 4T1 cells were plated under adherent (tissue culture-treated plate) and non-adherent conditions (poly-HEMA-coated plate). Cells were treated with DMSO or the indicated concentrations of PND-1186, harvested after 24, 48 and 72 h, and enumerated. Values are means (+/-SD) performed in triplicate (*p < 0.05; ***p < 0.0001 using ANOVA). (B) Cell cycle analysis as determined by propidium iodide (PI) staining and flow cytometry of 4T1 cells treated with PND-1186 for 72 h. Relative DNA content is indicated. Adherent cells treated with 1 μM PND-1186 show a slight increased in S and G_2/M phase cells. No significant differences were observed with suspended cells. Analyses are representative of two independent experiments. (C) PND-1186 promotes caspase-3 cleavage only in suspension. Lysates from adherent or suspended 4T1 cells treated for 24 h with DMSO or the indicated amount of PND-1186 were analyzed by immunoblotting with antibodies to pY397 FAK, total FAK, cleaved caspase 3 and GAPDH. (D) Flow cytometry was used to determine the percentage of annexin V-positive staining from adherent or suspended 4T1 cells treated for 24 h with DMSO or the indicated amount of PND-1186. Average values +/- SD were determined by triplicate analyses (*p < 0.05; ***p < 0.0001 using ANOVA).

4T1 cells, increasing concentrations (0.1 to 1.0 µM) of PND-1186 were added to adherent or suspended 4T1 cells and total cell numbers were enumerated after 24, 48 and 72 h (**Fig. 4A**). In adherent cells, no differences were observed at 24 or 48 h. However at 72 h, 1.0 µM PND-1186-treated cells were decreased in number and propidium iodide (PI) staining combined with flow cytometry analyses revealed a slight accumulation in the S and G_2/M phases of the cell cycle compared to DMSO control (**Fig. 4B**). In suspended 4T1 cells, all concentrations of PND-1186 reduced cell numbers at 48 h and this difference was significant ($p < 0.001$) for 0.1 µM PND-1186 at 72 h compared to DMSO (**Fig. 4A**). Interestingly, PI staining analyses of 1.0 µM PND-1186 treated cells in suspension did not reveal cell cycle differences (**Fig. 4B**). However, there was an accumulation of sub-diploid (1N) cells as detected by PI staining which is a marker of apoptosis in other cell types.[29] These results show that PND-1186 has limited effects on cell cycle progression and effects on total cell numbers may be associated with cell death.

To determine if PND-1186 is triggering suspended 4T1 cell apoptosis, lysates of adherent and suspended 4T1 cells treated with PND-1186 for 24 h and were analyzed by immunoblotting (**Fig. 4C**). PND-1186 at 0.1 µM was sufficient to inhibit FAK pY397 phosphorylation in adherent and suspended cells. Notably, the detection of cleaved caspase 3 was increased in PND-1186-treated suspended cells (maximal at 0.4 µM) but was not detectable in PND-1186 treated adherent cells (**Fig. 4C**). Caspase 3 cleavage is associated with caspase 3 activation and is an initiator of cell apoptosis.[30] As an independent verification of 4T1 cell apoptosis in suspension upon addition of PND-1186, cells were treated for 24 h and analyzed for annexin V binding by flow cytometry (**Fig. 4D**). In adherent conditions, only low levels of annexin V-positive cells were detected and this did not increase upon PND-1186 addition up to 1.0 µM. In contrast, suspended 4T1 control cells exhibited elevated annexin V staining and this was further increased to 50–60% annexin V positive staining upon 0.1 to 0.4 µM PND-1186 addition (**Fig. 4D**). Taken together, the triggering of 4T1 cell apoptosis under suspended conditions upon low level PND-1186 addition suggests that FAK activity may be essential for the survival of cells under anchorage-independent conditions. In contrast, the resistance of adherent 4T1 cells to high PND-1186 levels supports the notion that FAK activity is not essential for adhesion-associated cell survival.

PND-1186 inhibition of FAK and p130Cas tyrosine phosphorylation under spheroid growth conditions. It has been hypothesized that growing tumor cells as three dimensional (3D) multi-cellular spheroids in vitro mimics aspects of solid tumors compared to cells grown in two-dimensional monolayers.[31] As PND-1186 selectively promotes 4T1 cell apoptosis under suspended cell conditions (**Fig. 4**), 4T1 cells were cultured as 3D spheroids and increasing concentrations of PND-1186 (0.1 to 1.0 µM) were added for 72 h to determine effects on spheroid size (**Fig. 5A and B**). At 0.1 µM PND-1186, there was a ~3-fold reduction in average spheroid size and maximal effects were observed at 0.2 µM PND-1186. To date, no other FAK inhibitor
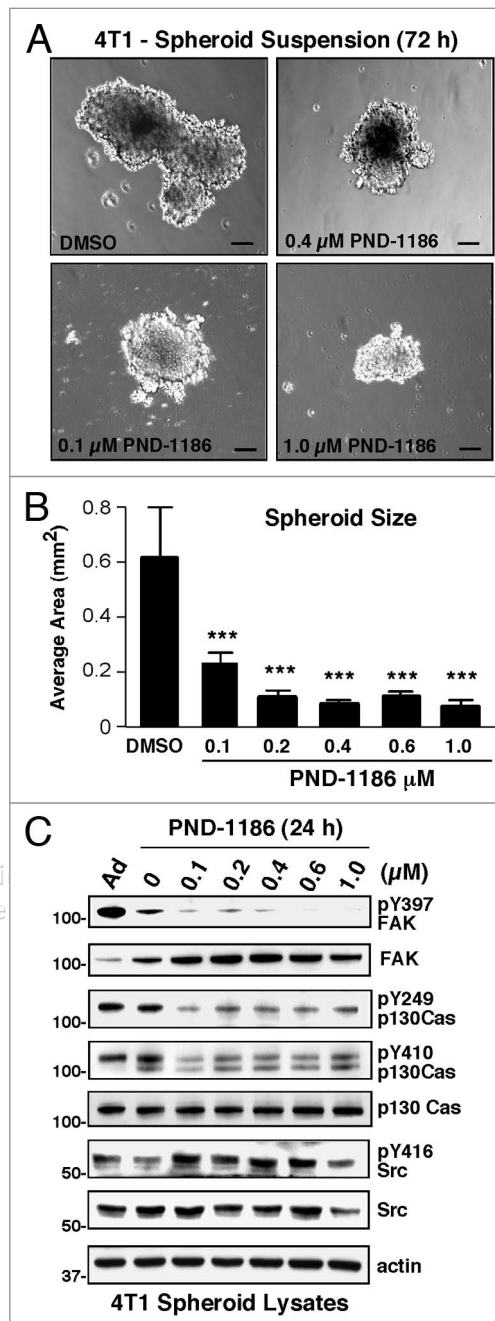

Figure 5. PND-1186 inhibits 4T1 spheroid growth and FAK-p130Cas phosphorylation in suspension. (A) Representative phase-contrast images of control non-adherent 4T1 spheroids (DMSO) and 4T1 spheroids in the presence of the indicated amount of PND-1186 for 72 h. Scale bar is 100 µm. (B) Spheroid size at 72 h (n = 40) was determined by area calculations using Image J from phase contrast images. Average values (+/-SD) are shown (***$p < 0.0001$ using ANOVA). (C) As spheroids, PND-1186 promotes FAK and p130Cas dephosphorylation. Adherent (Ad) untreated 4T1, suspended control (DMSO, 0) or PND-1186 treated 4T1 cell lysates were analyzed by immunoblotting with antibodies to pY397 FAK, FAK, pY249 p130Cas, pY410 p310Cas, p130Cas, pY416 Src, Src and actin.
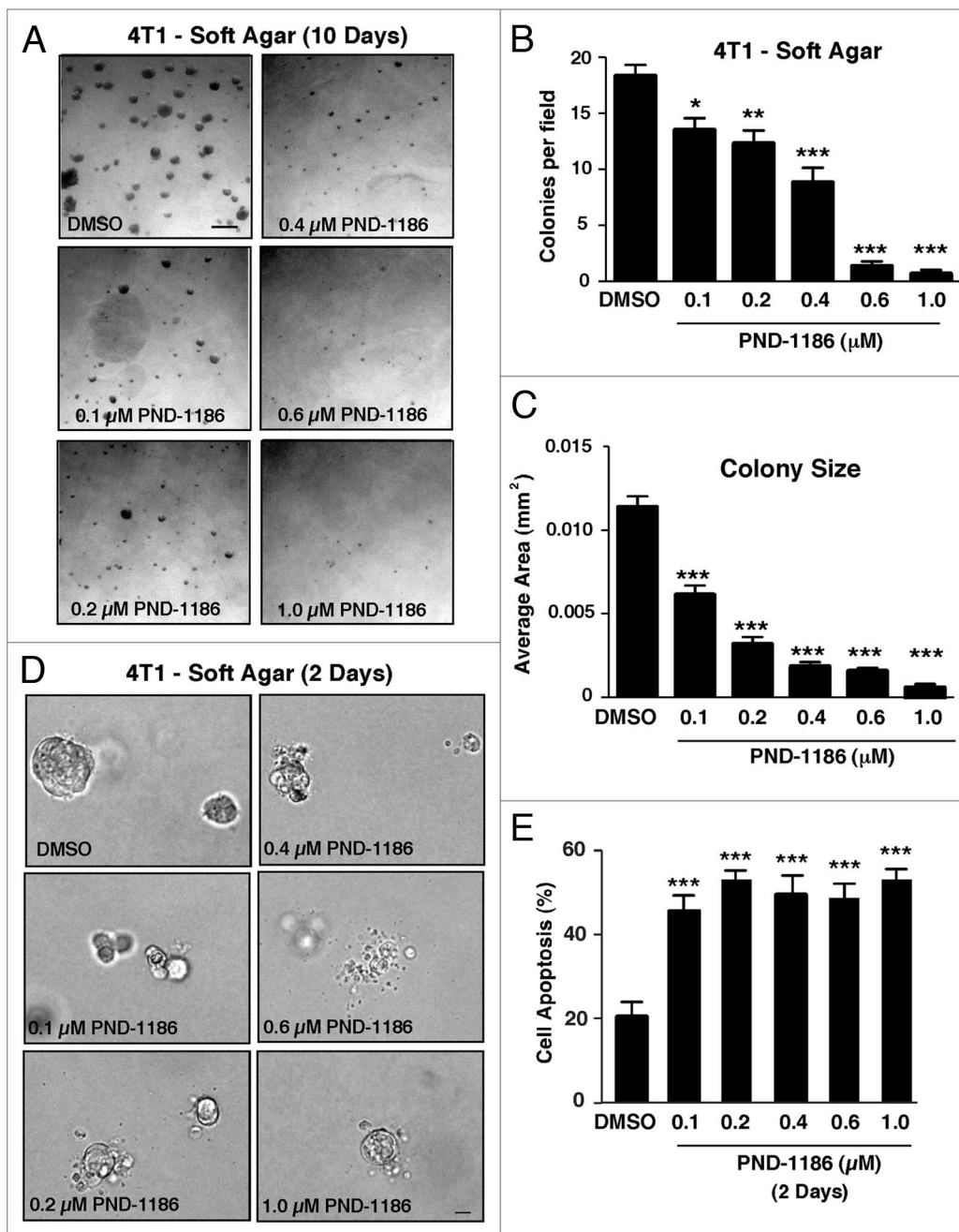
Figure 6. PND-1186 inhibition of 4T1 colony number and size in soft agar is associated with increased apoptosis. 4T1 cells were embedded in 0.3% agar. Vehicle (DMSO) or the indicated concentrations of PND-1186 were added and after 10 days, colonies were imaged by phase contrast microscopy (n = 10 images per condition). (A) Representative images of 4T1 colonies are shown, scale bar is 1 mm. (B) Average colonies per field and (C) average colony size after 10 days were calculated using Image J. Colony areas were determined from at least 200 colonies per condition. (D) Representative phase contrast images of soft agar 4T1 colony morphology after 48 h. Scale bar is 100 μm. (E) Apoptosis was quantified by visual inspection of at least 200 cells and was defined as the appearance of membrane blebbing or cell shrinkage. Ten fields per condition were observed and bars are means (+/-SD) from one experiment performed in triplicate. Significant difference between groups and DMSO control was determined by ANOVA (*$p < 0.05$; **$p < 0.001$; ***$p < 0.0001$).

has shown maximal inhibition of a biological response at sub-micromolar levels.

To determine specificity of PND-1186 FAK inhibition in 4T1 spheroids, immunoblotting was performed (**Fig. 5C**). The total level of FAK pY397 phosphorylation was reduced under 3D spheroid compared to adherent 4T1 conditions. No differences

were found for p130Cas pY249 or p130Cas pY410 phosphorylation in adherent versus 3D spheroid conditions (**Fig. 5C, lanes 1 and 2**). However, 0.1 μM PND-1186 potently inhibited FAK pY397, p130Cas pY249 and p130Cas pY410 phosphorylation in 4T1 spheroids (**Fig. 5C, lanes 3**). Increasing PND-1186 addition resulted in elevated total FAK levels, no change in p130Cas
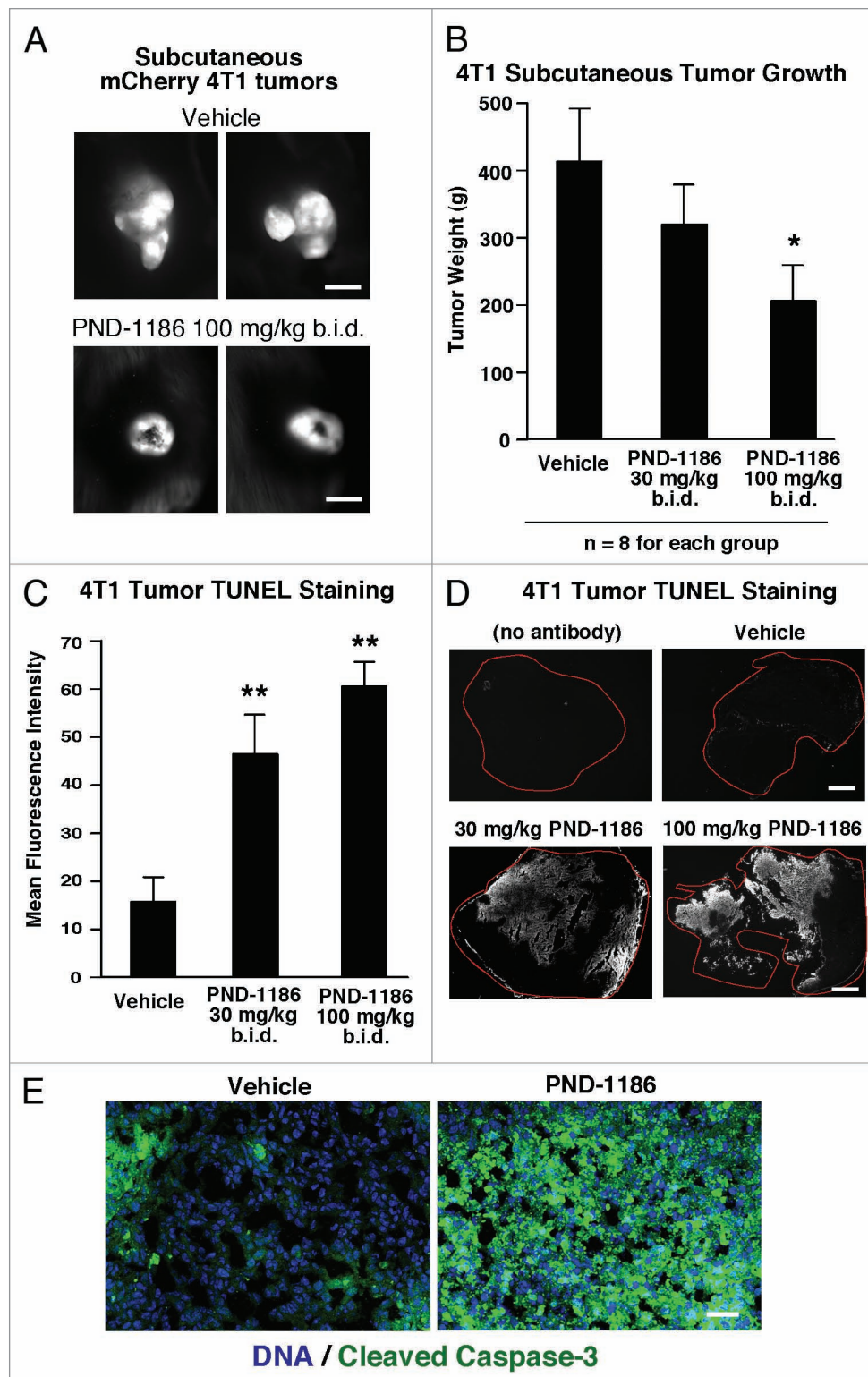
Figure 7. PND-1186 inhibits 4T1 subcutaneous tumor growth by induction of apoptosis. One million mCherry-labeled 4T1 cells were injected subcutaneously using BALB/c mice. After 8 days, mice received vehicle, 30 mg/kg PND-1186, or 100 mg/kg PND-1186 twice a day (b.i.d.). Tumors were harvested after 5 days of treatment. (A) Representative OV-100 fluorescent images of mCherry-labeled 4T1 tumors in situ. Necrotic cores are visible in 100 mg/kg PND-1186 treated tumors. Scale bar is 1 cm. (B) Effect of PND-1186 on final tumor weight. Values are means (+/-SD). (C) Quantification of average fluorescent TUNEL staining intensity (+/-SD) in medial tumor sections (n = 10 per group) as determined using Image J. For (B and C), significant differences between vehicle and PND-1186 treatment groups was determined using ANOVA (*p < 0.05; **p < 0.001). (D) Representative images of TUNEL-stained tumor sections (whole tumor section is outlined in red). Scale bar is 0.2 mm. (E) Evaluation of cell-associated (Hoechst DNA staining, blue) and cleaved caspase-3 staining in control or 100 mg/kg PND-1186-treated tumors. Scale bar is 0.1 mm.
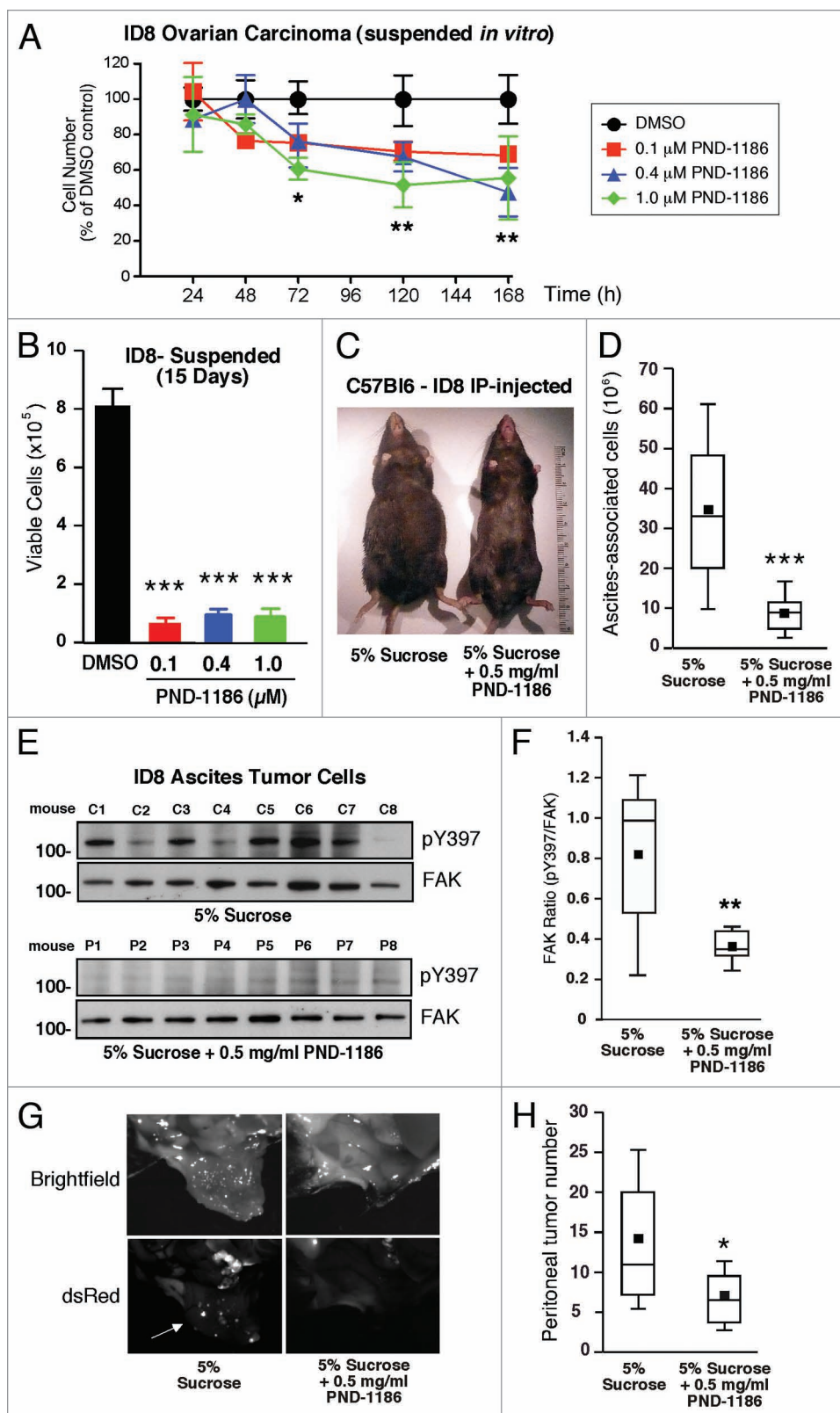
Figure 8. PND-1186 inhibits ovarian carcinoma tumor growth. (A and B) ID8 cells were plated under non-adherent conditions (poly-HEMA-coated plate) in the presence of DMSO or the indicated amounts of PND-1186 and enumerated from 24 to 168 h as indicated. (B) Viable cell numbers were determined by trypan blue exclusion and counting using a Vi-Cell analyzer after 15 days. (C) Representative images of C57Bl6 mice injected (intraperitoneal, IP) with dsRed-labeled ID8 cells after 46 days provided 5% sucrose (control) or 0.5 mg/ml PND-1186 in 5% sucrose ad libitum as drinking water for 30 days. (D) Ascites was collected, peritoneal cavity washed with saline, and total cell numbers enumerated from ID8 IP-injected mice. (E) Evaluation of FAK phosphorylation in ascites-associated cells as determined by anti-FAK followed by phospho-specific anti-FAK pY397 immunoblotting. (F) Ratio of pY397 phosphorylated FAK to total FAK levels in ascites cells as determined by densitometry using Image J (n = 8 per group). (G) Representative brightfield and fluorescent images of peritoneal tissue from C57Bl6 mice IP-injected with dsRed-labeled ID8 cells after 46 days provided 5% sucrose (control) or 0.5 mg/ml PND-1186. Arrow indicates dsRed-positive tumor nodules in control mice. (H) Peritoneal-associated tumors were quantified by counting (n = 8 per group). Values are means (+/-SD) performed in triplicate and significance was determined by ANOVA (*$p < 0.05$; **$p < 0.001$, ***$p < 0.0001$ versus control). Box-and-whisker diagrams show the distribution of the data: square, mean; bottom line, 25th percentile; middle line, median; top line, 75th percentile; and whiskers, 5th or 95th percentiles.

4T1 spheroids differs from the lack of PND-1186 effects on 4T1 cells as a two-dimensional (2D) monolayer (**Fig. 2A**). As FAK interactions with p130Cas have been shown to promote cell survival,[25,32] and PND-1186 inhibitory effects on downstream targets of FAK are selectively revealed when cells are cultured under anchorage-independent or 3D conditions, our results support the hypothesis that FAK phosphorylation of targets such as p130Cas may facilitate the survival of 4T1 cells in 3D conditions.

PND-1186 decreases soft agar colony number and size at nanomolar concentrations. It can be argued that anchorage-independent 3D spheroids do not fully recapitulate the architecture

expression, and sustained inhibition of FAK and p130Cas tyrosine phosphorylation (**Fig. 5C**). There was no change in either Src pY416 or Src expression levels in adherent, spheroid or PND-1186-treated spheroid 4T1 cells (**Fig. 5C**). Importantly, the inhibition of p130Cas phosphorylation by PND-1186 in

of nascent growing breast tumors that have some type of provisional scaffold. Thus, 4T1 cells were grown as colonies in soft agar and the effects of PND-1186 addition evaluated (**Fig. 6**). By 10 days, PND-1186 addition inhibited both the total number and size of 4T1 soft agar colonies in a dose-dependent manner (**Fig. 6A–C**). Similar results were obtained when PND-1186 was added 4 days after the establishment of 4T1 cells in soft agar (**Suppl. Fig. 2**). At 0.2 µM PND-1186, 4T1 soft agar colony size was inhibited 77% (**Fig. 6C**) and this corresponded to increased 4T1 cell apoptosis (>50%) as determined by membrane blebbing and cell shrinkage (**Fig. 6D and E**). Taken together, our results support the hypothesis that PND-1186 does not work as a general cytotoxic drug, but selectively and potently interferes with the survival of cells in a 3D environment.

PND-1186 inhibits 4T1 subcutaneous tumor growth by induction of apoptosis. To determine the sensitivity of 4T1 tumor growth to PND-1186 administration, mCherry fluorescently-labeled 4T1 cells were grown subcutaneously in BALB/c mice (**Fig. 7**). After allowing eight days for primary tumor establishment, vehicle or PND-1186 at 30 mg/kg or at 100 mg/kg was administered every 12 h (twice-daily, b.i.d.) for 5 days after which time, mCherry 4T1 tumors were visualized in situ followed by extraction and weighing (**Fig. 7A and B**). Whereas vehicle-treated 4T1 tumors were brightly fluorescent, generally multi-lobed and had become invasive to the surrounding tissues, tumors in mice treated with 100 mg/kg PND-1186 contained dark non-fluorescent centers, were generally rounded, and were loosely adherent to sub-dermal tissues (**Fig. 7A**). 100 mg/kg PND-1186 treatment significantly reduced final 4T1 tumor weight 2-fold (n = 8, p < 0.05) whereas 30 mg/kg PND-1186 slightly reduced final tumor weight but was not significantly different compared to control (n = 8, p > 0.05). To determine if the loss of mCherry fluorescence in the center of 100 mg/kg PND-1186 tumors was associated with increased cell apoptosis, medial sections were analyzed by TUNEL (**Fig. 7C and D**) staining. Both 30 and 100 mg/kg administration of PND-1186 significantly increased tumor TUNEL staining compared to vehicle-treated controls (**Fig. 7D**). As elevated cleaved caspase-3 staining was also found in the tumors of PND-1186-treated mice (**Fig. 7E**), these results parallel our in vitro analyses and show that PND-1186 promotes apoptosis of 4T1 cells in 3D conditions resulting in the inhibition of tumor growth in vivo.

PND-1186 inhibits ovarian carcinoma tumor growth in vivo. During ovarian carcinoma tumor cell progression, cells can dissociate from the primary tumor and grow as multi-cellular spheroids within the peritoneal space.[33] As PND-1186 selectively promotes 4T1 breast carcinoma apoptosis in 3D environments, PND-1186 effects on murine ID8 ovarian carcinoma cell growth were evaluated in vitro and in vivo (**Fig. 8**). In suspended cell culture as spheroids, 0.1, 0.4 and 1.0 µM PND-1186 significantly inhibited ID8 cell number at 72 h (**Fig. 8A**) and resulted in a dramatic reduction in viable cells after 15 days (**Fig. 8B**). To determine if low levels of PND-1186 could affect ID8 growth in vivo, dsRed fluorescently-labeled ID8 cells were intraperitoneally-injected into C57Bl6 mice and after 11 days, mice were provided 5% sucrose (control) or 0.5 mg/ml PND-1186 in 5% sucrose in

lieu of drinking water on an ad libitum basis. No adverse effects and no body weight loss were noted with PND-1186 administration. After 30 treatment days, mice with PND-1186 in the drinking water did not exhibit swollen abdomens as did control mice (**Fig. 8C**). This corresponded with a lower number of ascites-associated cells (**Fig. 8D**) and the >2-fold inhibition of FAK pY397 by 0.5 mg/ml PND-1186 administration compared to 5% sucrose controls (**Fig. 8E and F**). In addition to inhibiting ascites-associated ID8 spheroid growth, PND-1186-treated mice showed significantly fewer tumor nodules within the peritoneal space as detected by in vivo dsRed fluorescence imaging (**Fig. 8G and H**). These results show that low level PND-1186 administration inhibits the growth of ovarian carcinoma cells in vitro and in vivo. The selective effects on PND-1186 in promoting apoptosis of cells in three dimensional environments points to a novel role for FAK activity in generating anchorage-independent survival signals.

Discussion

Increased expression and phosphorylation of FAK is associated with tumor progression and malignancy.[14] For this reason, and because of the known cell migration promoting properties of FAK, there has been considerable interest in developing inhibitors for clinical use.[6] TAE-226 inhibits FAK and other kinases which complicates interpretations of the mechanism(s) of action.[19] However, PF-562,271 has high specificity for FAK and the related Pyk2 kinase and can prevent human xenograft growth in immuno-compromised mice.[17] This may occur through increased apoptosis of vascular cells within tumors[17] or via the suppression of stromal angiogenesis.[23,24]

Herein, we present the characterization of a new 2,4-diaminopyridine-based reversible small molecule inhibitor to FAK. PND-1186 has an IC_{50} of 1.5 nM to recombinant FAK and exhibits high specificity to FAK in vitro at 0.1 µM as determined by Millipore KinaseProfiler analyses (**Fig. 1**). In 2D monolayer cell culture, 0.1 µM PND-1186 potently inhibits FAK pY397 phosphorylation without affects on p130Cas or c-Src tyrosine phosphorylation (**Fig. 2**). In contrast, the Abl/Src inhibitor desatinib blocks p130Cas and Src tyrosine phosphorylation events without effects on FAK. As anticipated, PND-1186 prevents cell motility (**Fig. 3**) and time-lapse microscopic imaging revealed that 4T1 breast cancer cells continued to undergo cell division in the presence of 1.0 µM PND-1186 (see **Suppl. Videos 1 and 2**). Importantly, 0.1 µM PND-1186 was sufficient to promote 4T1 breast carcinoma and ID8 ovarian carcinoma cell apoptosis when cells were grown under suspended, spheroid or soft-agar conditions (**Figs. 4–6 and 8**). This was associated with the inhibition of both FAK and p130Cas but not Src tyrosine phosphorylation (**Fig. 5**), supporting the hypothesis that a selective FAK-p130Cas survival pathway facilitates 3D tumor cell growth.

A connection between FAK signaling and cell survival was first noted using antisense knockdown or micro-injection of antibodies to FAK[34,35] and has been attributed to loss of integrin-associated survival signals.[36] To this end, FAK has been linked to matrix survival signaling through the activation of a variety

of downstream pathways.[25] However, adhesion-dependent roles for FAK in promoting cell survival may be distinct from the role of FAK in promoting 3D cell survival in tumor cells. Notably, 2D adherent 4T1 or ID8,[37] cell cultures did not demonstrate a dependency on FAK activity for survival as the same cells did under 3D conditions (**Fig. 4**). In our studies, FAK inhibition was validated by pY397 blot and by assessment of FAK substrate sites on p130Cas. FAK activity was blocked at similar concentrations among cells grown in 2D or 3D conditions. Although recent studies have implicated a kinase-independent survival role for FAK in p53 tumor suppressor inhibition,[38] ID8 cells possess intact p53 and 4T1 cells are p53-null, yet both cells exhibit sensitivity to low level PND-1186 treatment in undergoing apoptosis. Thus, our results support the notion that PND-1186 inhibition of FAK affects p53-independent pathways within 3D-cultured cells.

One key difference between 2D and 3D conditions was p130Cas tyrosine phosphorylation. PND-1186 inhibited p130Cas phosphorylation in 3D conditions but not 2D culture conditions. This suggests that interaction with a rigid substrate can either stabilize phosphorylated p130Cas or facilitate its phosphorylation by an alternative tyrosine kinases such as Src as previously shown for force-dependent signaling.[39] Although our findings with regard to a specific FAK-p130Cas signaling connection in 3D remain correlative, p130Cas phosphorylation promotes apoptosis resistance of cells in suspension[40] and the survival of tumor cells in 3D.[41,42] Mechanistically, FAK Y397 phosphorylation is also important in facilitating inside-out integrin activation.[43] Thus, in 3D spheroids, FAK activity may facilitate integrin interactions with adhesion molecules on neighboring tumor cells, thus promoting cell survival signaling. Such a role is also consistent with the multiple linkages between p130Cas and proteins affecting cytoskeletal actin remodeling.[27] These interactions would be expected to suppress pro-death signals by ligating integrins and suppressing of caspase 3 activation.[44] Interestingly, PND-1186 inhibition of p130Cas tyrosine phosphorylation and increased 4T1 tumor cell apoptosis was independent of effects on Akt phosphorylation-activation.[45] The survival pathway potentially downstream of p130Cas tyrosine phosphorylation remains under investigation.

Our analyses have also extended in vitro observations to 4T1 and ID8 tumor growth inhibition associated with increased cell apoptosis (**Figs. 7 and 8**). Interestingly, we did not observe effects on tumor vascularity in the subcutaneous 4T1 tumors (unpublished observations). One might argue that aggressive 4T1 tumor growth, which secretes many inflammatory and angiogenic growth factors, could be sufficient to override anti-angiogenic effects of FAK inhibition. However, PND-1186 inhibitory effects on ID8 ovarian tumor growth in situ as peritoneal ascites is likely also mediated through an angiogenesis-independent effect. Thus, although FAK inhibition may influence angiogenesis, our data collectively indicate that such activity may not be essential for inhibition of tumor growth in vivo. Rather, the induction of apoptosis among cells growing in a 3D environment appeared key.

Our results also raise the possibility that FAK activation may provide a selective advantage to tumor cells growing in a 3D microenvironment. As hepatocellular carcinoma growth in 3D was associated with increased FAK levels,[46] and increased FAK expression is linked to tumor progression,[4-6] FAK signaling may facilitate cell growth in 3D environments typically seen in malignancy. As our preclinical studies show that PND-1186 has low intrinsic toxicity to mice and is efficacious at low concentrations administered ad libitum in promoting tumor apoptosis, there is significant merit for testing PND-1186 as an anti-cancer therapy in the clinic.

Materials and Methods

Chemical synthesis. PND-1186 was identified through high-throughput kinase activity screens and conventional medicinal chemistry approaches. The structure will be published elsewhere (Koenig M, manuscript in preparation). PND-1186 was synthesized and prepared as a HCl salt as described in a patent application.[47] For in vivo assays, PND-1186 was dissolved in water (solubility = 22 mg/ml).

Baculovirus FAK catalytic domain and in vitro kinase assays. The FAK catalytic domain region (411–686) was generated by polymerase chain reaction using the primers 5'-CGA TCG AAT TCT CGA CCA GGG ATT ATG AGA TTC A-3', 5'-TAG CTG TCG ACT TAC TGC ACC TTC TCC TCC TCC AGG-3', cloned into pGEX4T as a fusion with GST, and moved into the pAcG2T baculovirus expression vector (Pharmingen, Baculogold). Virus clones were identified by plaque assays and amplified. For protein expression, SF9 cells were transduced at a multiplicity of infection of 2–5 pfu/cell and cultured at 27°C for 48 h. Glutathione agarose affinity chromatography were used to purify GST-FAK (411–686) followed by size fractionation using hiload 16/60 Superdex chromatography (GE Healthcare). Protein was concentrated and stored frozen in 50 mM Tris pH 8.0, 150 mM NaCl, 1 mM Na orthovanadate, 0.5 mM EDTA, 0.5 mM EGTA, 0.1% β-mercaptoethanol and 20% glycerol. Purity was estimated at >90% by SDS-PAGE. GST-FAK in vitro kinase activity was measured and compared to His-tagged FAK 411–686 (Millipore) using the K-LISA screening kit (Calbiochem) and poly(Glu:Tyr) (4:1) copolymer (P0275, Sigma) as a substrate immobilized on microtiter plates. IC_{50} values were determined with various concentrations of test compounds in a buffer containing 50 µM ATP and 10 mM $MnCl_2$, 50 mM HEPES (pH 7.5), 25 mM NaCl, 0.01% BSA and 0.1 mM Na orthovanadate for 5 min at room temperature. Serial diluted compounds at ½-Log concentrations (starting at 1 µM) were tested in triplicate. Substrate phosphorylation was measured using horseradish peroxidase-conjugated anti-pTyr antibodies (PY20, Santa Cruz Biotechnology) with spetrophotometic color quantitation. IC_{50} values were determined using the Hill-Slope Model. Kinase selectivity profiling was performed by using the KinaseProfiler service (Millipore).

Reagents and cells. Antibodies to β-actin (AC-17) were from Sigma-Aldrich. Antibodies to Src (Src-2) were from Santa Cruz Biotechnology. Antibodies to FAK (4.47) were from Millipore. Site and phospho-specific antibodies to pY249 p130Cas, pY410 p130Cas, pY416 Src and anti-cleaved caspase-3 were from Cell

Signaling Technology. Anti-pY397 FAK and TOPRO-3 were from Invitrogen. Anti-GAPDH (glyceraldehyde-3-phosphate dehydrogenase) was from Chemicon, bovine plasma fibronectin was from Sigma, and Dasatinib and PP1 were from LC Laboratories and Calbiochem, respectively. 4T1 murine mammary carcinoma cells and MDA-MB-231 human breast carcinoma cells were from American Type Culture Collection. ID8 mouse ovarian carcinoma cells were from Katherine Roby.[48] Cells were cultured in Dulbecco's modified Eagle's medium supplemented with 10% fetal bovine serum (FBS), 1 mM non-essential amino acids, 2 mM glutamine, 100 U/ml penicillin and 100 µg/ml streptomycin. For in vitro studies, PND-1186 was dissolved in dimethyl sulfoxide (DMSO) and stored at -80°C until time of use. Final experimental DMSO concentration was between 0.1% to 0.2%. The coding sequence for red fluorescent mCherry or dsRed proteins (Clontech) were subcloned into the lentiviral expression vector (pCDH-MSC1, System Biociences) and recombinant lentivirus was produced as described.[13] Transduced 4T1 or ID8 cells were enriched by fluorescence-activated cell sorting (FACSAria, Becton-Dickinson) to acquire stable population of cells.

Anchorage-dependent, spheroid and soft agar cell growth assays. Cells (2×10^5) were plated per 35 mm well under adherent (tissue culture-treated) and non-adherent conditions (poly-HEMA-coated) in 6-well plates (Costar) in growth media. Between 24 and 168 h, all cells were collected, a single cell suspension was prepared by limited trypsin-EDTA treatment, and viable cells were enumerated by trypan blue staining and counting (ViCell XR, Beckman). For spheroid area determination, cells were imaged after 72 h in phase contrast using an Olympus IX51 microscope. Area was calculated using Image J software (version 1.43). For soft agar assays, 48-well plates were coated with a 1:4 mix of 2% agar (EM Science) in 0.2 ml growth media (bottom layer). 5×10^4 cells were plated per well (in triplicate) in a mixture of 0.3% agar in 0.2 ml growth media (top layer). After agar solidification, 0.2 ml growth media was added containing DMSO or PND-1186 (final concentration for 0.6 ml). In separate experiments, PND-1186 was added after 4 days. After 10 days, colonies were imaged in phase contrast, enumerated by counting 9 fields (3 fields per well), and total area determined using Image J. For all analyses, experimental points were performed in triplicate and were experiments were repeated at least two times.

Immunoblotting. Protein extracts of cells were made using lysis buffer containing 1% Triton X-100, 1% sodium deoxycholate, and 0.1% SDS and were separated by 4–12% SDS-PAGE (sodium dodecyl sulfate polyacrylamide gel electrophoresis) and sequential immunoblotting performed as described.[13] Relative expression levels and phospho-specific antibody reactivity were measured by densitometry analyses of blots using Image J.

Cell migration assays. Serum-stimulated chemotaxis using Millicell (12 mm diameter with 8 µm pores; Millipore) chambers were performed as described previously.[49] Both sides of membrane were coated with fibronectin (10 µg/ml) and chemotaxis was stimulated by addition of 10% FBS to the lower chamber. Data points represent cell counts (9 fields) from three migration chambers from at least two independent experiments. For scratch-wound closure motility assays, cells were seeded onto fibronectin-coated (10 µg/ml) glass bottom 12 well plates (MatTek) and serum starved (0.5% FBS) for 16 h. Cells were wounded with a pipette tip, washed with phosphate-buffered salin (PBS), and replenished with 10% FBS media with or without FAK inhibitor (1 µM). Time-lapse series was obtained by acquiring images at 10 min intervals for up to 22 h, at 37°C with humidity and CO_2 regulation using a 10X objective on an automated stage (Olympus IX81). Cell trajectories and distance traveled were measured by tracking nucleus position over time using Image J.

Cell growth and apoptosis assays. For cell growth analyses, adherent or suspended cells were treated with PND-1186 for the indicated times, collected as a single cell suspension by limited trypsin treatment, fixed with 70% ethanol, collected by centrifugation and washed with PBS. Cell pellets were resuspended in 300 µl of PBS containing propidium iodide (PI) (10 µg/ml), DNAse-free RNAse (100 µg/ml, Qiagen), and then incubated at 37°C with agitation for 1 h. Samples were analyzed by flow cytometry (FACSCalibur, Becton-Dickinson) and cell cycle analyses were performed by ModFit LT3.2 software (Verity software house). Hypodiploid DNA content as a measure of cell apoptosis was detected by PI staining as described.[29] For cell apoptosis analyses, adherent or suspended cells were treated with PND-1186 and collected as above, stained for phycoerythrin (PE)-conjugated annexin V binding and 7-amino-actinomycin (7-AAD) reactivity (BD Pharmingen), and analyzed within 1 h by flow cytometry. Quadrant gates were positioned based on cell autofluorescence (negative) staurosporine-treated (positive) controls. Apoptosis was calculated to be the percent of annexin V-positive cells. In the soft agar assays, apoptosis was quantified by visual inspection of at least 200 cells and was defined as the appearance of membrane blebbing or cell shrinkage. Apoptosis was also detected by appearance of cleaved caspase-3 antibody reactivity in protein lysates by immunoblotting.

Detection of apoptosis in tumors. Fresh tumors were snap-frozen in Optimal Cutting Temperature (OCT) compound (Tissue Tek), thin sectioned (7 µM) using a cryomicrotome (Leica 3050S) and mounted onto glass slides. Sections were fixed with 3% paraformaldehyde, permeabilized in PBS containing 0.1% Triton for 3 min, and blocked with 8% goat serum in PBS for 60 min at RT. For activated caspase-3 detection, sections were incubated with cleaved caspase-3 antibody (1:200 diluted in 2% goat serum in PBS) for 18 h at 4°C, washed with PBS, and incubated with fluorescein isothiocyanate conjugated anti-rabbit and TOPRO-3 (blue) for DNA detection. Sections were imaged on a Nikon Eclipse C1 confocal microscope with a 1.4 NA 60X oil objective, with a 30 µm pinhole setting, and analyzed using EZ-C1 3.50 software (Nikon). Tumor apoptosis was also measured by terminal deoxynucleotidyl transferase dUTP nick end labeling (TUNEL) staining using the tetramethylrhodamine (TMR) kit as per the manufacturer's instructions (Roche). Bright field and fluorescent images of whole tumor sections were obtained using Zeiss M2-Bio Stereo microscope equipped with INFINITY1-3C: digital color camera and a 4X objective.

Mouse tumor studies. Six to eight week old female C57Bl6 and BALB/c mice were obtained from Harlan Laboratories (Indianapolis, IN) and housed in pathogen-free conditions,

according to the guidelines of the Association for the Assessment and Accreditation for Laboratory Animal Care, International. All in vivo studies were carried out under an approved institutional experimental animal care and use protocol. Growing tumor cells were harvested by limited trypsinization, washed in PBS, and counted using a ViCell XR (Beckman) prior to injection. Cell viability as measured by trypan blue exclusion was >95%. For subcutaneous tumor growth, 1×10^6 mCherry-labeled 4T1 cells in 100 µl PBS were injected into the hindflank of Balb/C mice. After 8 days, mice with equal volume tumors (as measured using vernier calipers and determined by length x width^2/2) were grouped (n = 8 per group) and PND-1186 solubilized in polyethylene glycol 400 (PEG400) in PBS (1:1) was injected (100 µl) subcutaneously in the neck region at 30 mg/kg or 100 mg/kg every 12 hours. Control animals received PEG400:PBS injections and at 13 days, tumors were imaged in situ using an Olympus OV100 Intravital Fluorescence Molecular Imaging System, tumors were excised and weighed, half was frozen in OCT, and half was solubilized in protein lysis buffer for FAK phosphorylation analyses. For ID8 ovarian carcinoma tumor growth, 0.8 mL of 1×10^7 ID8 cells in PBS was intraperitoneal injected into C57Bl6 mice. After 11 days, 0.5 mg/mL PND-1186 dissolved in 5% sucrose in water was provided for drinking and control mice received 5% sucrose (n = 8 per group). Administration continued ad libitum for 30 days after which mice were euthanized, ascites fluid collected, cells obtained by centrifugation (2,000 rpm for 5 min), cell volume measured by pipet, and then solubilized in protein lysis buffer for immunoblotting analyses.

Statistical analyses. GraphPad Prism (v5.0a) was used to determine significant differences between groups using one-way analysis of variance (ANOVA) followed by the Tukey post hoc test. Differences between pairs of data were ascertained using an unpaired two-tailed student's t-test or a two-tailed Mann-Whitney test.

Note

Supplementary materials can be found at: www.landesbioscience.com/supplement/TanjoniCBT9-10-Sup.pdf

References

1. Schlaepfer DD, Hauck CR, Sieg DJ. Signaling through focal adhesion kinase. Prog Biophys Mol Biol 1999; 71:4-6.
2. Mitra SK, Hanson DA, Schlaepfer DD. Focal adhesion kinase: in command and control of cell motility. Nat Rev Mol Cell Biol 2005; 6:56-68.
3. Tomar A, Schlaepfer DD. Focal adhesion kinase: switching between GAPs and GEFs in the regulation of cell motility. Curr Opin Cell Biol 2009; 21:676-83.
4. McLean GW, Carragher NO, Avizienyte E, Evans J, Brunton VG, Frame MC. The role of focal-adhesion kinase in cancer—a new therapeutic opportunity. Nat Rev Cancer 2005; 5:505-15.
5. Zhao J, Guan JL. Signal transduction by focal adhesion kinase in cancer. Cancer Metastasis Rev 2009; 28:35-49.
6. Parsons JT, Slack-Davis J, Tilghman R, Roberts WG. Focal adhesion kinase: targeting adhesion signaling pathways for therapeutic intervention. Clin Cancer Res 2008; 14:627-32.
7. Benlimame N, He Q, Jie S, Xiao D, Xu YJ, Loignon M, et al. FAK signaling is critical for ErbB-2/ErbB-3 receptor cooperation for oncogenic transformation and invasion. J Cell Biol 2005; 171:505-16.
8. Luo M, Fan H, Nagy T, Wei H, Wang C, Liu S, et al. Mammary epithelial-specific ablation of the focal adhesion kinase suppresses mammary tumorigenesis by affecting mammary cancer stem/progenitor cells. Cancer Res 2009; 69:466-74.
9. Provenzano PP, Inman DR, Eliceiri KW, Beggs HE, Keely PJ. Mammary epithelial-specific disruption of focal adhesion kinase retards tumor formation and metastasis in a transgenic mouse model of human breast cancer. Am J Pathol 2008; 173:1551-65.
10. Lahlou H, Sanguin-Gendreau V, Zuo D, Cardiff RD, McLean GW, Frame MC, et al. Mammary epithelial-specific disruption of the focal adhesion kinase blocks mammary tumor progression. Proc Natl Acad Sci USA 2007; 104:20302-7.
11. Pylayeva Y, Gillen KM, Gerald W, Beggs HE, Reichardt LF, Giancotti FG. Ras- and PI3K-dependent breast tumorigenesis in mice and humans requires focal adhesion kinase signaling. J Clin Invest 2009; 119:252-66.
12. van Nimwegen MJ, Verkoeijen S, van Buren L, Burg D, van de Water B. Requirement for focal adhesion kinase in the early phase of mammary adenocarcinoma lung metastasis formation. Cancer Res 2005; 65:4698-706.
13. Mitra SK, Lim ST, Chi A, Schlaepfer DD. Intrinsic focal adhesion kinase activity controls orthotopic breast carcinoma metastasis via the regulation of urokinase plasminogen activator expression in a syngeneic tumor model. Oncogene 2006; 25:4429-40.
14. Mitra SK, Schlaepfer DD. Integrin-regulated FAK-Src signaling in normal and cancer cells. Curr Opin Cell Biol 2006; 18:516-23.
15. Shi Q, Hjelmeland AB, Keir ST, Song L, Wickman S, Jackson D, et al. A novel low-molecular weight inhibitor of focal adhesion kinase, TAE226, inhibits glioma growth. Mol Carcinog 2007; 46:488-96.
16. Slack-Davis JK, Martin KH, Tilghman RW, Iwanicki M, Ung EJ, Autry C, et al. Cellular characterization of a novel focal adhesion kinase inhibitor. J Biol Chem 2007; 282:14845-52.
17. Roberts WG, Ung E, Whalen P, Cooper B, Hulford C, Autry C, et al. Antitumor activity and pharmacology of a selective focal adhesion kinase inhibitor, PF-562,271. Cancer Res 2008; 68:1935-44.
18. Golubovskaya VM, Nyberg C, Zheng M, Kweh F, Magis A, Ostrov D, et al. A small molecule inhibitor, 1,2,4,5-benzenetetraamine tetrahydrochloride, targeting the y397 site of focal adhesion kinase decreases tumor growth. J Med Chem 2008; 51:7405-16.
19. Liu TJ, LaFortune T, Honda T, Ohmori O, Hatakeyama S, Meyer T, et al. Inhibition of both focal adhesion kinase and insulin-like growth factor-I receptor kinase suppresses glioma proliferation in vitro and in vivo. Mol Cancer Ther 2007; 6:1357-67.
20. Halder J, Lin YG, Merritt WM, Spannuth WA, Nick AM, Honda T, et al. Therapeutic efficacy of a novel focal adhesion kinase inhibitor TAE226 in ovarian carcinoma. Cancer Res 2007; 67:10976-83.
21. Golubovskaya VM, Virnig C, Cance WG. TAE226-Induced apoptosis in breast cancer cells with overexpressed Src or EGFR. Mol Carcinog 2007; 47:222-34.
22. Hochwald SN, Nyberg C, Zheng M, Zheng D, Wood C, Massoll NA, et al. A novel small molecule inhibitor of FAK decreases growth of human pancreatic cancer. Cell Cycle 2009; 8:2435-43.
23. Lim S-T, Mikolon D, Stupack DG, Schlaepfer DD. FERM control of FAK function: Implications for cancer therapy. Cell Cycle 2008; 7:2306-14.
24. Weis SM, Lim ST, Lutu-Fuga KM, Barnes LA, Chen XL, Göthert JR, et al. Compensatory role for Pyk2 during angiogenesis in adult mice lacking endothelial cell FAK. J Cell Biol 2008; 181:43-50.
25. Zouq NK, Keeble JA, Lindsay J, Valentijn AJ, Zhang L, Mills D, et al. FAK engages multiple pathways to maintain survival of fibroblasts and epithelia: differential roles for paxillin and p130Cas. J Cell Sci 2009; 122:357-67.
26. Wu L, Bernard-Trifilo JA, Lim Y, Lim ST, Mitra SK, Uryu S, et al. Distinct FAK-Src activation events promote alpha5beta1 and alpha4beta1 integrin-stimulated neuroblastoma cell motility. Oncogene 2008; 27:1439-48.
27. Defilippi P, Di Stefano P, Cabodi S. p130Cas: a versatile scaffold in signaling networks. Trends Cell Biol 2006; 16:257-63.

28. Sieg DJ, Hauck CR, Ilic D, Klingbeil CK, Schaefer E, Damsky CH, et al. FAK integrates growth-factor and integrin signals to promote cell migration. Nat Cell Biol 2000; 2:249-56.

29. Nicoletti I, Migliorati G, Pagliacci MC, Grignani F, Riccardi C. A rapid and simple method for measuring thymocyte apoptosis by propidium iodide staining and flow cytometry. J Immunol Methods 1991; 139:271-9.

30. Mazumder S, Plesca D, Almasan A. Caspase-3 activation is a critical determinant of genotoxic stress-induced apoptosis. Methods Mol Biol 2008; 414:13-21.

31. Friedrich J, Seidel C, Ebner R, Kunz-Schughart LA. Spheroid-based drug screen: considerations and practical approach. Nat Protoc 2009; 4:309-24.

32. Almeida EA, Ilic D, Han Q, Hauck CR, Jin F, Kawakatsu H, et al. Matrix survival signaling: from fibronectin via focal adhesion kinase to c-Jun NH(2)-terminal kinase. J Cell Biol 2000; 149:741-54.

33. Shield K, Ackland ML, Ahmed N, Rice GE. Multicellular spheroids in ovarian cancer metastases: Biology and pathology. Gynecol Oncol 2009; 113:143-8.

34. Frisch SM, Vuori K, Ruoslahti E, Chan-Hui PY. Control of adhesion-dependent cell survival by focal adhesion kinase. J Cell Biol 1996; 134:793-9.

35. Hungerford JE, Compton MT, Matter ML, Hoffstrom BG, Otey CA. Inhibition of pp125FAK in cultured fibroblasts results in apoptosis. J Cell Biol 1996; 135:1383-90.

36. Stupack DG, Cheresh DA. Get a ligand, get a life: integrins, signaling and cell survival. J Cell Sci 2002; 115:3729-38.

37. Lim ST, Miller NL, Nam JO, Chen XL, Lim Y, Schlaepfer DD. PYK2 inhibition of p53 as an adaptive and intrinsic mechanism facilitating cell proliferation and survival. J Biol Chem 2009; 285:1743-53.

38. Ilic D, Almeida EA, Schlaepfer DD, Dazin P, Aizawa S, Damsky CH. Extracellular matrix survival signals transduced by focal adhesion kinase suppress p53-mediated apoptosis. J Cell Biol 1998; 143:547-60.

39. Sawada Y, Tamada M, Dubin-Thaler BJ, Cherniavskaya O, Sakai R, Tanaka S, et al. Force sensing by mechanical extension of the Src family kinase substrate p130Cas. Cell 2006; 127:1015-26.

40. Cho SY, Klemke RL. Extracellular-regulated kinase activation and CAS/Crk coupling regulate cell migration and suppress apoptosis during invasion of the extracellular matrix. J Cell Biol 2000; 149:223-36.

41. Cabodi S, Tinnirello A, Di Stefano P, Bisaro B, Ambrosino E, Castellano I, et al. p130Cas as a new regulator of mammary epithelial cell proliferation, survival and HER2-neu oncogene-dependent breast tumorigenesis. Cancer Res 2006; 66:4672-80.

42. Provenzano PP, Keely PJ. The role of focal adhesion kinase in tumor initiation and progression. Cell Adh Migr 2009; 3:347-50.

43. Michael KE, Dumbauld DW, Burns KL, Hanks SK, Garcia AJ. FAK Modulates Cell Adhesion Strengthening via Integrin Activation. Mol Biol Cell 2009; 20:2508-19.

44. Frisch SM. Caspase-8: fly or die. Cancer Res 2008; 68:4491-3.

45. Walsh C, Tanjoni I, Uryu S, Nam JO, Mielgo A, Tomar A, et al. Oral delivery of PND-1186 FAK inhibitor decreases spontaneous breast to lung metastasis in pre-clinical tumor models. Cancer Biol Ther 2010; 9.

46. Wu YM, Tang J, Zhao P, Chen ZN, Jiang JL. Morphological changes and molecular expressions of hepatocellular carcinoma cells in three-dimensional culture model. Exp Mol Pathol 2009; 87:133-40.

47. Liang C, Koenig M, He Y, Holmberg P. Inhibitors of Focal Adhesion Kinase. World Intellectual Property Organization 2008; WO2008115369.

48. Roby KF, Taylor CC, Sweetwood JP, Cheng Y, Pace JL, Tawfik O, et al. Development of a syngeneic mouse model for events related to ovarian cancer. Carcinogenesis 2000; 21:585-91.

49. Lim Y, Lim ST, Tomar A, Gardel M, Bernard-Trifilo JA, Chen XL, et al. PyK2 and FAK connections to p190Rho guanine nucleotide exchange factor regulate RhoA activity, focal adhesion formation and cell motility. J Cell Biol 2008; 180:187-203.